12-2007

# Techniques for Improving the Performance of Coupled Oscillator Arrays

Venkatesh Seetharam
*Clemson University*, vseetha@clemson.edu

# TECHNIQUES FOR IMPROVING THE PERFORMANCE OF COUPLED OSCILLATOR ARRAYS

---

A Dissertation
Presented to
the Graduate School of
Clemson University

---

In Partial Fulfillment
of the Requirements for the Degree
Doctor of Philosophy
Electrical Engineering

---

by
Venkatesh Seetharam
December 2007

---

Accepted by:
L. Wilson Pearson, Committee Chair
Xiao-Bang Xu
William R. Harrell
James Bruce Rafert

ABSTRACT

Coupled oscillator arrays (COAs) have excellent synchronization properties that can be utilized to develop a low cost alternative to phased array systems for beam steering applications. The primary concerns in implementing the COA architecture are the sensitivity to cell-to-cell component variation and poor phase noise performance. Wide injection locking range oscillators reduce the sensitivity to component variation but degrade the array phase noise performance.

The objective of this dissertation is to alleviate the concerns hindering the application of COAs by employing techniques to realize COAs with wide mutual injection locking ranges (MILR), improved phase noise characteristics and beam steering capabilities. In the first manuscript [1], a dually resonant oscillator configuration, which offers the flexibility of mutual coupling at different locations, is optimized for low *Q* and used to fabricate two three-element COAs - one in which oscillators are mutually coupled at the drain terminal and another in which oscillators are mutually coupled at the gate terminal. In both arrays, the oscillator elements are coupled with coupling phases of $2\pi$, $3\pi$ and $4\pi$ radians at 3.75 GHz. For both arrays the coupling phase that resulted in broadside operation yielded the largest MILRs, whereas the coupling phase that caused the array to lock with a limited range resulted in out of phase synchronization of the oscillator elements.

In the second paper, the behavior of COAs in the strongly coupled regime is analyzed. For large coupling strengths, the resonant nature of the coupling network

[1] This dissertation is assembled from three papers prepared for journal submission.

increases resulting in the breakdown of the broadband condition. A five-element COA operating at 3.75 GHz was fabricated and the MILR, phase noise and oscillator amplitude and phase variation were measured for coupling strengths varying from 0.5 to 2.5. A two-fold improvement in the MILR and 25 dB improvement in the array free-running phase noise is achieved. The beam steering capability of strongly coupled arrays is also presented. Strong coupling causes the amplitudes of the oscillator elements to grow toward the extremes of the array. When strongly coupled arrays are employed in a phased array system the side lobe level will be undesirably large. Tapering of the array amplitude distribution is utilized to achieve reduction in the side lobe level. The beam steering capability of strongly coupled arrays is also presented.

In the third paper, the multiport injection technique is shown as a means to enhance the beam steering and phase noise performance of the array. For a nine element COA operating at 10 GHz, the maximum beam steering ($15.6^{\circ}$) is obtained when oscillators #4 and #6 are simultaneously injection locked with a $174^{\circ}$ phase difference. Two, three and four port injection locking of the array is performed and the measured phase noise performance is compared with theory. Regardless of the number of oscillators simultaneously injection locked, the best phase noise performance is observed when the oscillators nearest to the center element are chosen for injection locking. By injection locking the oscillators nearest to the center element the same phase noise performance is obtained with fewer injection- locked oscillators.

# DEDICATION

I dedicate this work to my beloved parents who taught me the importance of education, hard work and positive thinking in one's life. Their love, sacrifices and motivation alone provided me the strength to pursue my dreams and achieve success.

ACKNOWLEDGMENTS

I would like to thank my advisor, Dr. L. Wilson Pearson, for the confidence that he has shown in my scholastic ability and giving me the opportunity to work on the fascinating topic of coupled oscillator arrays. I am extremely grateful for all the support, motivation and guidance that he has extended during the course of my graduate studies. I extend my appreciation to Dr. Xiao-Bang Xu, Dr. James Rafert and Dr. W. Rod Harrell for serving on my committee, the time they spent reviewing my work and their invaluable suggestions.

I would like to thank Dr. Ronald Pogorzelski of Jet Propulsion Laboratory (Caltech) for the numerous fruitful technical conversations and his encouragement. I would like to thank my fellow graduate students Chris Tompkins, Joel Simoneau, Xiong Wang, Michael Frye, Haiyan Yang and Adam Schreiber for their suggestions and assistance. I would especially like to acknowledge Chris Tompkins, whose mentoring helped accelerate my understanding of coupled oscillator arrays.

TABLE OF CONTENTS

Page

Table of Contents (Continued)

LIST OF TABLES

LIST OF FIGURES

List of Figures (Continued)

List of Figures (Continued)

# INTRODUCTION

Coupled oscillator arrays (COAs) are suitable for use in beam steering applications due to their excellent synchronization ability. When single-device oscillators are fabricated in an array, loaded with antennas and coupled together, synchronization through mutual injection locking results in a coherent beam of radiation [I.1]-[I.5]. The direction of the beam is controlled by the free-running frequency distribution of the array [I.6]-[I.8]. Hence beam steering can be achieved without the use of phase shifters. COAs also provide higher powers at millimeter wave frequencies than conventional power-combining techniques. The use of COAs would be cost-effective and highly beneficial to traditional phased array systems such as radar due to the simplified control architecture. However, the sensitivity to cell-to-cell component variation [I.6], [I.9]-[I.11] and poor phase noise performance has diminished the attractiveness of COAs.

The seminal work in injection-locked oscillators was performed by Adler [I.12]. Adler presented the theoretical description of an oscillator driven by a small signal injection source, where the amplitude of the injected signal is small compared to the amplitude of the driven oscillator. He established a relation between the driven oscillator and the injected signal. The relation is given as

$$\frac{d\left(\theta-\theta_{inj}\right)}{dt}=\omega_o-\omega_{inj}+\frac{\omega_0}{2Q}\frac{A_{inj}}{A_0}\sin\left(\theta_{inj}-\theta\right), \tag{I.1}$$

where $A_0, \theta, \omega_o, Q$ are the amplitude, phase, free-running frequency, and quality factor of the oscillator and $A_{inj}, \theta_{inj}, \omega_{inj}$ are the amplitude, phase and frequency of the injected signal. The term $\frac{\omega_0}{2Q}\frac{A_{inj}}{A_0}$ represents the locking-range ($\Delta\omega_{\max}$), the maximum frequency range over which locking can occur. Adler's work serves as the base from which COA analysis was derived.

Later, Kurokawa extended the analysis to account for large signal injection locking [I.13]. Assuming the amplitude and phase of the oscillator to be slowly varying functions of time, he performed a first-order approximation of the time derivative of these quantities to derive the generalized dynamic equations for injection locked oscillators. He showed that these equations reduce to (I.1) for the case of small signal injection locking. Kurokawa also computed the injection locking bandwidth [I.14] and phase noise [I.15]. He also discussed the idea of designing broadband oscillators by reducing the external *Q* of the oscillator [I.14]. He noted that an oscillator tuned with a single resonance is not always adequate, but often the *Q* may be further reduced by designing a multiple resonant circuit. He showed that the locking range of a double-resonant circuit characterized by quality factors $Q_1$ and $Q_2$ is calculated as

$$\Delta\omega_{\max} = \frac{\omega_0}{2\left(Q_1 - Q_2\right)}\frac{A_{inj}}{A_o} \tag{I.2}$$

As $Q_2$ approaches $Q_1$, the locking range increases, but the noise also increases substantially.

Stephan and Morgan applied the oscillator injection-lock theory to an array of oscillators which are coupled through a network [I.1], [I.16]. The equations developed by Kurokawa were extended to describe a linear array of coupled oscillators, and the coupled oscillator theory was formed. They found that synchronizing a linear array of oscillators by means of a proper coupling network causes the oscillators to operate in-phase with each other. Hence the signals can be added coherently in a monolithic power combining scheme or, by driving radiating elements, in air.

A phased array can be realized by unilaterally injection locking the oscillators. One idea is to injection lock all the oscillators to a single external signal. In another method, the oscillators are injection locked in cascade and the free-running frequency of each oscillator can then be tuned individually to obtain the desired phase distribution in the array. From phase noise viewpoint, locking to a single external signal is preferred. Birkland and Itoh [I.3] built a 4x4 FET oscillator array at 6 GHz in which each oscillator is injection locked by signals with equal frequency and phase from a power divider. The free-running frequency of each oscillator was tuned to that of the injection signal. The authors were able to form a uniform phase-front, which placed the main beam at the broadside direction.

Al Ani, Cullen and Forrest [I.17] realized the first beam-steering array by phase-locking each of the four oscillators to an injection source. The required phase shift was obtained through detuning the free-running frequency of each oscillator. Lin, Chew, and Itoh [I.18] employed the second scheme to achieve large beam-scanning ranges. The unilateral injection locking was implemented by using amplifiers between the oscillators,

which helped to increase the locking-range and reduce the perturbation to oscillator performance.

Mutual injection locking allows a progressive phase shift between the oscillators with a much simpler circuitry. Stephan and Morgan [I.16] showed that when the end elements of a one-dimensional COA are injection locked, the phase difference between these signals is evenly divided among the array elements resulting in a linear phase progression along the array. The two end oscillators are injection-locked to two external sources whose phase difference is controlled by a phase-shifter. The total realizable phase progression is limited to less than $360^\circ$ due to the phase shifter and the phase shift is divided equally among all oscillators in the array. As a result, the inter-element phase difference decreases linearly as the element number increases making this design impractical for a phased array system.

York and his colleagues extended the work of Stephan and explored many aspects of COA theory. York developed the analysis of an oscillator array with an arbitrary coupling network, described in terms of N-port circuit parameters [I.8]. York showed that an inter-element phase shift in the range of $-90^\circ$ to $+90^\circ$ can be realized easily by detuning the free-running frequencies of the two edge oscillators equally in opposite directions [I.6]. Since the two end oscillators are detuned in opposite directions by the same amount, the ensemble frequency does not change. The total phase shift is not restricted to $360^\circ$and increases proportionally with the number of elements in the array. York also showed that small deviations in the oscillator's free-running frequencies could affect the phase distribution. However, this shortcoming can be overcome by increasing

the locking bandwidth of the oscillators. Based on York's theory, several researchers have explored different methods to implement COA systems. Transmission line coupling [I.19] and slotline coupling [I.20], [I.21] of active microstrip antennas were investigated. Another research group [I.22] considered adjusting the coupling phase of the edge oscillators as opposed to detuning their free-running frequencies. The design obviates the problems caused due to deviations in free-running frequencies but added complexity in the design and control circuitry. The use of phase-locked loop (PLL) in the coupling network was explored by Martinez and Compton [I.23]. This methodology simultaneously improves the locking range and the phase noise, although the author's do not discuss the phase noise performance.

York's contribution to COAs is invaluable. He and his colleagues evaluated the phase noise in a free-running COA as well as in an array with one oscillator injection locked to an external signal [I.24]-[I.26] . Achieving wide locking-range required for the frequency detuning scheme comes at the expense of phase noise. Using a PLL coupling scheme [I.27], [I.28] provides a wide-locking range low noise option, but increases the cost, complexity and power consumption of COA systems. Tompkins and Pearson introduced the use of mutli-port injection locking method to improve the phase noise of coupled oscillator arrays [I.29].

Pogorzelski and York derived a continuum diffusion model for the phase dynamic equation of the coupled oscillator array by using a small argument approximation [I.30]-[I.32]. They noted that the solution to the phase dynamic equation is the discritized equivalent of Poisson's equation of electrostatics. Identifying the frequency distribution

of the edge elements with charge density, they compared the phase distribution of the array to the electrostatic potential. The continuum model helps to determine beam settling times and can be employed for quick computations on large two dimensional arrays.

The possibility of multi-moding in arrays was discovered by Stephan [I.33]. He also presented a simple analysis which helped to understand and eliminate the undesired modes. Itoh was the first researcher to analyze in detail the problems of multi-moding and stability in strongly coupled arrays [I.34]-[I.36]. He proposed a modal analysis to determine the possible modes in an array. With the help of the average potential theory, he devised criteria for stability of each mode. He showed that all the undesired modes could be suppressed by placing resistors at appropriate locations in the coupling network and thereby ensured oscillation in the power combining mode. Chang *et. al* [I.37] discuss the influence of the resonant nature of the oscillator equivalent circuit on the stable modes of coupled-oscillator system. They observed significant differences in the dynamics of parallel and series equivalent oscillators for a particular coupling scheme, leading to different stable-phase distributions for each case.

Pearson and his colleagues have further investigated the effect of fabrication tolerances on COA performance. Shen and Pearson present a thorough analysis of the phase error and beam-pointing error due to variations in the free-running frequencies of the oscillators in a COA and devise a post fabrication calibration method for beam pointing correction [I.9], [I.10]. Wang and Pearson present a technique to lower the open loop phase slope of the oscillator through optimization to provide wide injection locking-ranges [I.38]. This technique utilizes the virtual ground method devised by Alechno

[I.39], [I.40]. The open loop gain and phase slope can be obtained through an open loop analysis [I.41]. Tompkins and Pearson further improved the technique to reduce the tolerance to variation in oscillator free-running frequencies [I.29].

The complicated amplitude and phase dynamic equations that York developed are simplified when the coupling network has a slower frequency variation than the oscillator. Pogorzelski developed an expression to compute the frequency variation of the coupling network [I.42]. In his work, he provides a thorough analysis and design of a typical broadband coupling network for both one and two dimensional arrays. Lynch and York investigated the issue of narrowband coupling [I.43]. They noted that narrowband coupling reduces the probability of array synchronization and decreases the oscillator's locking range.

Numerical and CAD based analysis of injection locked oscillators have been pursued by several researchers. Dixon, *et. al* [I.44] developed a time-domain analysis of injection locked MESFET oscillators while Rizzoli, *et. al* [I.45] applied the harmonic-balance method. Collado and his colleagues extended the application of harmonic-balance method to synthesize COAs [I.46], [I.47]. Shumaker and Eisenstein [I.48] developed an elaborate numerical model to analyze large signal injection locking in both unidirectionally and bidirectionally coupled oscillators.

The objective of this dissertation is to alleviate the concerns hindering the application of COAs by employing techniques to realize COAs with wide mutual injection locking ranges, improved phase noise characteristics and beam steering capabilities. The first manuscript [I.49] shows that type of resonance, series or parallel,

presented to the coupling network by the oscillators depends upon the coupling point in the oscillator circuit. The manuscript also discusses the effect of coupling phase on the mutual injection locking range and the mode of array operation for different coupling locations.

The second manuscript[I.50] employs strongly coupled oscillator arrays to obtain simultaneous improvement in the mutual injection locking range and phase noise performance. A theoretical analysis of strongly coupled arrays is presented and the array amplitude and phase variation with coupling strength is computed. The theory is verified with experiments performed on a five-element COA operating at 3.75 GHz. Tapering of the oscillator amplitudes is utilized to achieve reduction in the side lobe level. The beam steering capability of strongly coupled arrays is also presented.

The third manuscript employs multiport injection locking technique on a nine-element COA operating at 10 GHz to show enhanced beam steering and phase noise performance. By moving the injection locking locations progressively towards the center element, improvements in beam steering and phase noise performance are observed. The measured results are compared with the theory.

The conclusions consist of the key results and findings from each manuscript. Appendix A presents the finite difference approximation technique used for solving first-order non-linear coupled differential equations.

References

[I.1] K. D. Stephan, "Inter-injection-locked oscillators for power combining and phased arrays," *IEEE Trans. Microwave Theory and Tech.*, vol. 34, pp. 1017-1025, Oct. 1986.

[I.2] W. A. Morgan and K. D. Stephan, "X-band experimental model of a millimeter-wave inter-injection-locked phased array system," *IEEE Trans. Antennas and Propagation*, vol. 36, pp. 1641-1645, Nov. 1988.

[I.3] J. Birkland and T. Itoh, "A 16-element quasi-optical FET oscillator power combining array with external injection locking," IEEE Trans. Microwave Theory and Tech., vol. 40, pp. 475-481, Mar. 1992.

[I.4] A. Mortazawi, H. D. Foltz, and T. Itoh, "A periodic second harmonic spatial power-combining oscillator," *IEEE Trans. Microwave Theory and Tech.*, vol. 40, pp 851–856, May 1992.

[I.5] R. A. York, C. Compton, "Quasioptical power-combining using mutually synchronized oscillator arrays," *IEEE Trans. Microwave Theory and Tech.*, vol. 39, pp. 1000-1009, Jun. 1991.

[I.6] R. A. York, "Nonlinear-analysis of phase-relationships in quasi-optical oscillator arrays," *IEEE Trans. Microwave Theory and Tech.*, vol.41, pp. 1799-1809, Oct. 1993.

[I.7] P. Liao, R. A. York, "A new phase-shifterless beam-scanning technique using arrays of coupled oscillators," *IEEE Trans. Microwave Theory and Tech.,* vol. 41, pp. 1810-1815, Oct. 1993.

[I.8] R. A. York, P. Liao, J. J. Lynch, "Oscillator array dynamics with broad-band n-port coupling network*," IEEE Trans. Microwave Theory and Tech.*, vol. 42, pp. 2040-2045, Nov. 1994.

[I.9] J. Shen and L. W. Pearson, "Oscillator reproducibility consideration in coupled oscillator phase-steering arrays," *IEEE MTT-S International Microwave Symposium Digest*, vol. 2, pp. 827-830, Jun. 2000.

[I.10] J. Shen and L. W. Pearson, "The phase error and beam-pointing error in coupled oscillator beam-steering arrays," *IEEE Transactions on Antennas and Propagation,* vol. 53, pp. 386-393, Jan. 2005.

[I.11] X. Wang and L. W. Pearson, "Design of coupled-oscillator arrays without a posteriori tuning," *IEEE Trans. Microwave Theory and Tech.,* vol. 53 , pp. 410-413, Jan. 2005.

[I.12] R. Adler, "A study of locking phenomena in oscillators," *Proc. IRE*, vol. 34, pp.351-357, Jun. 1946.

[I.13] K. Kurokawa, "Injection-locking of solid-state microwave oscillators," *Proc. IEEE*, vol. 61, pp.1386-1409, Oct. 1973.

[I.14] K. Kurokawa, "Some basic characteristics of broadband negative resistance oscillator circuits," *Bell Systems Tech. Journal*, vol. 48, pp.1937-1955, Oct. 1971.

[I.15] K. Kurokawa, "Noise in synchronized oscillators," *IEEE Trans. Microwave Theory and Tech.*, vol. 16, pp. 234-240, Apr. 1968.

[I.16] K. D. Stephan and W. A. Morgan, "Analysis of inter-injection-locked oscillators for integrated phased arrays," *IEEE Trans. Antennas and Propagation,* vol. 35, pp.771-781, Jul. 1987.

[I.17] A.H. Al-Ani, A.L.Cullen, and J.R.Forrest, "A phase-locking method for beam steering in active array antennas," *IEEE Trans. Microwave Theory and Tech.*, vol. 22, pp. 698-703, June 1974.

[I.18] J. Lin, S. T. Chew, and T. Itoh, "A unilateral injection-locking type active phased array for beam scanning," *IEEE MTT-S International Microwave Symposium Digest,* vol. 2, pp. 1231-1234, May 1994.

[I.19] R. Ispir, S. Nogi, M. Sanagi, and K. Fukui, "Transmission-line coupling of active microstrip antennas for one- and two-dimensional phased arrays," *IEICE Trans. Electron*., vol. E80-C, pp.1211-1220, Sep. 1997.

[I.20] C. Mun, C. H. Kang, H. K. Park, and Y. J. Yoon, "The active phased array antennas coupled through slotlines," *IEEE MTT-S International Microwave Symposium Digest*, vol. 2, pp. 1069-1072, Jun. 1997.

[I.21] T. Y. Lee, Y. J. Yoon, and G. S. Jang, "A study on the two-dimensional slotline coupling structure for active planar array antennas," *IEEE AP-S Symposium Digest,* vol. 3, pp. 1398-1400, Jun. 1998.

[I.22] J. H. Hwang and N. H. Myung, "A new beam-scanning technique by controlling the coupling angle in a coupled oscillator array," *IEEE Microwave and Guided Wave Letters*, vol. 8, pp. 191-193, May 1998.

[I.23] R. D. Martinez and R. C. Compton, "Electronic beam-steering of active arrays with phase-locked loops," *IEEE Microwave and Guided Wave Letters*, vol. 4, pp. 166-168, Jun. 1994.

[I.24] X. Cao and R. A. York, "Phase noise reduction in scanning oscillator arrays," *IEEE MTT-S International Microwave Symposium Digest*, vol. 2, pp. 769-772, May 1995.

[I.25] H. C. Chang, X. Cao, and R. A. York, "Phase noise in coupled oscillators: theory and experiment," *IEEE Trans. Microwave Theory and Tech.,* vol. 45, pp. 604-615, May 1997.

[I.26] H. C. Chang, X. Cao, U. K. Mishra, and R. A. York, "Phase noise in externally injection-locked oscillator arrays," *IEEE Trans. Microwave Theory and Tech.*, vol. 45, pp. 2035-2042, Nov. 1997.

[I.27] H. C. Chang, A. Borgioli, P. Yeh, and R. A. York, "Analysis of oscillators with external feedback loop for improved locking range and noise reduction," *IEEE Trans. Microwave Theory and Tech*., vol. 47, pp. 1535-1543, Aug. 1999.

[I.28] H. C. Chang, "Analysis of coupled phase-locked loops with independent oscillators for beam control active phased arrays," *IEEE Trans. Microwave Theory and Tech*., vol. 52, pp. 1059-1066, Mar. 2004.

[I.29] C. M. Tompkins, "Coupled oscillator array design and the use of multiport injection locking for improved performance," Ph. D. Dissertation, Clemson University, August 2006.

[I.30] R. J. Pogorzelski and R. A. York, "A simplified theory of coupled oscillator array phase control," *IEEE AP-S International Symposium Digest*, pp. 324–327, Jul. 1997.

[I.31] R. J. Pogorzelski, P. F. Maccarini, and R. A. York, "Continuum modeling of the dynamics of externally injection-locked coupled oscillator arrays," *IEEE Trans. Microwave Theory and Tech*., vol. 47, pp. 471-478, Apr. 1999.

[I.32] R. J. Pogorzelski, P. F. Maccarini, and R. A. York, "Continuum modeling of the dynamics of coupled oscillator arrays for phase-shifterless beam-scanning," *IEEE Trans. Microwave Theory and Tech*., vol. 47, pp. 463-470, Apr. 1999.

[I.33] K. D. Stephan and S. L. Young, "Mode stability of radiation-coupled inter-injection-locked oscillators for integrated phased arrays," *IEEE Trans. Microwave Theory and Tech.*, vol. 36, pp. 921-924, May 1988.

[I.34] J. Lin, and T. Itoh, "A 4X4 spatial power-combining array with strongly coupled oscillators in multi-layer structure," *IEEE MTT-S International Microwave Symposium Digest*, vol. 2, pp. 607-610, May 1993.

[I.35] J. Lin, and T. Itoh, "Two-dimensional quasi-optical power-combining arrays using strongly coupled oscillators," *IEEE Trans. Microwave Theory and Tech.*, vol. 42, pp. 734-741, Dec. 1994.

[I.36] S. Nogi, J. Lin, and T. Itoh, "Mode analysis and stabilization of a spatial power combining array with strongly coupled oscillators," *IEEE Trans. Microwave Theory and Tech.*, vol. 41, pp. 1827-1837, Oct. 1993.

[I.37] H. C. Chang, E. S. Shapiro, R. A. York, "Influence of oscillator equivalent circuit on the stable modes of parallel coupled oscillators," *IEEE Trans. On Microwave Theory and Tech*., MTT-45, pp. 1232-1239, Aug. 1997.

[I.38] X. Wang, "Design of wide-injection-locking- range oscillator elements for coupled oscillator arrays", Ph.D Dissertation, Clemson University, May 2003.

[I.39] S. Alechno, "Analysis method characterizes microwave oscillators—Part 1," *Microwaves & RF*, pp. 82-86, Nov 1997.

[I.40] S. Alechno, "The virtual ground in oscillator analysis- A practical example," *Applied Microwave and Wireless*, pp.44-53, Jul. 1999.

[I.41] M. Randall and T. Hock, "general oscillator characterization using linear open-loop s-parameters," *IEEE Trans. Microwave Theory and Tech*., vol. 49, pp. 1094-1100, Jun 2001.

[I.42] R. J. Pogorzelski, "On the design of coupling networks for coupled oscillator arrays," *IEEE Trans. Antennas and Propagation*, vol. 51, pp.794-801, April 2003.

[I.43] J. J. Lynch and R. A. York, "Synchronization of oscillators coupled through narrow band networks," *IEEE Trans. Microwave Theory and Tech.*, vol. 49, pp. 237-249, Feb. 2001.

[I.44] J. Dixon, E. Bradley and Z. B. Popovic, "Nonlinear time-domain analysis of injection-locked microwave MESFET oscillators", *IEEE Trans. Microwave Theory and Tech*., vol. 45, pp. 1050-1057, July 1997.

[I.45] V. Rizzoli, A. Neri and D. Masotti, "The application of harmonic-balance methodology to the analysis of injection locking", *IEEE Microwave Theory and Tech. Digest*, pp 1591-1594, 1992.

[I.46] A. Collado, F. Ramirez and J. P. Pascual, "Harmonic-balance analysis and synthesis of coupled-oscillator arrays", *IEEE Microwave and Wireless Components and Letters*, Vol. 14, No.5, May 2004.

[I.47] A. Suarez, A. Collado and F. Ramirez, "Harmonic-balance techniques for the design of coupled-oscillator systems in both unforced and injection-locked operation", *IEEE Microwave and Wireless Components and Letters*, Vol. 14, No.5, May 2004.

[I.48] E. Shumakher and G. Eisenstein, "On the noise properties of injection-locked oscillators", *IEEE Trans. On Microwave Theory and Tech*., vol. 52, pp. 1523-1537, May 2004.

[I.49] V. Seetharam, C. M. Tompkins and L. Wilson Pearson, “Effect of coupling network length on COA performance”, *IEEE AP-S International Symposium and URSI National Radio Science Meeting*, pp. 384, 2006.

[I.50] V. Seetharam, L. Wilson Pearson, “Analysis of strong coupling in coupled oscillator arrays”, *CNC/UNSC and North American Radio Science Meeting,* Ottawa, Canada, July 2006.

EFFECT OF COUPLING PHASE ON MUTUAL INJECTION LOCKING RANGE IN COUPLED OSCILLATOR ARRAYS

**Abstract— The performance of a coupled oscillator array depends critically on the coupling network. Determination of the optimal coupling phase depends on the oscillator equivalent circuit and the location of mutual coupling between the oscillators. In this paper, the authors examine the effects of coupling phase on the mutual injection locking range. Three element coupled oscillator arrays (COAs) are mutually coupled at two different locations, with each coupling location presenting a different resonance to the coupling network, and the optimal coupling phase required to generate a linear phase shift in the range of -90° to 90° is determined. For each coupling location, when the coupling phase is off by 180°, the arrays were shown to lock with a limited range and operate in the undesired mode.**

## I. Introduction

The coupling network design is a critical part of coupled oscillator array design. Pogorzelski [1.1] details the design of nearest neighbor coupling networks for coupled oscillator arrays (COAs). The design of the coupling network depends on the resonant nature of the oscillators as well. It has been shown that the coupling phase required to generate a linear phase shift in the range of -90° to 90°depends on the type of oscillator resonant equivalent circuit [1.2].

Wide injection locking range oscillators have excellent synchronization properties and tolerance to fabrication errors and therefore are attractive for use in COAs. Wang and Pearson presented an optimization technique to design oscillators for wide injection

locking ranges by lowering the *Q* of the oscillators [1.3]. In order to take advantage of the benefits of low Q oscillators in a COA, one injection locks the array externally to a low phase noise source, thereby ensuring low phase noise at the outputs of each oscillator cell in the array [1.4]. Methods to improve the locking ranges were reported by [1.5]. In this paper, the effect of coupling phase on the injection locking range and mode of operation of COAs employing low *Q* oscillators is examined. The optimization technique developed by Wang and Pearson is employed in the design of the wide injection locking range oscillators [1.3]. In Section II, the coupling phase required for in-phase synchronization for different locations of mutual coupling is discussed. We extend the theory developed by York [1.6], [1.7] and Pogorzelski [1.1] to derive the required coupling phase for mutual coupling on a resistor, capacitor and inductor for an oscillator presenting a series resonance to the coupling network. We show that when an oscillator with a series resonant equivalent circuit is coupled on a capacitor or an inductor, the required coupling phase is identical to that of a parallel resonant oscillator. Section III is devoted to showing the effect of coupling phase on the mutual injection locking range by mutually coupling the oscillator elements at different locations in a transistor oscillator configuration.

## II. Oscillator Array Dynamics and Coupling Networks

### A. Array Dynamics and Coupling Phase

The amplitude and phase dynamics of a coupled oscillator system as shown in Fig. 1.1 can be completely modeled by first-order coupled non-linear differential equations [1.6].

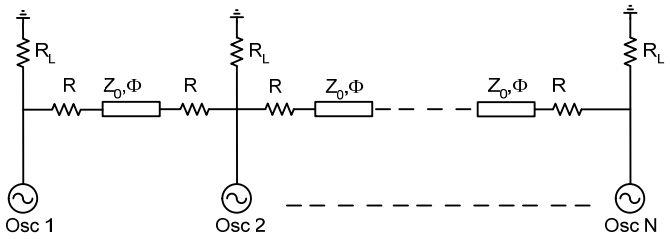

Fig. 1.1 An N-element coupled oscillator array.

The inter-oscillator coupling is characterized by coupling strength and coupling phase, which are the magnitude and phase components of the complex coupling coefficient. The locking range is defined as the maximum range over which the free-running frequencies of the oscillators can deviate collectively from the ensemble frequency and be able to attain a mutually locked state. The mathematical expression for the locking range is:

$$\Delta\omega_{lock} = \frac{\kappa_0 \omega_i}{2Q}, \tag{1.1}$$

where $\kappa_0$ is the magnitude of the complex coupling coefficient and is denoted as the coupling strength and $\omega_i$ and $Q$ are the oscillator free-running frequency and quality factors respectively.

From (1.1), it follows that oscillators with wide injection locking ranges have low $Q$. A large $\kappa_0$ indicates a large locking range. However, a large $\kappa_0$ causes strong coupling between the oscillator elements resulting in variations in the amplitude of oscillator outputs [1.8]. Moreover, a large $\kappa_0$ causes the coupling network to present a significant load to the oscillator [1.1]. Strong coupling ( $\kappa_0 > 0.5$ ) between the oscillator elements is desirable as long as other coupling features are not compromised. The broadband condition given by [1.7] simplifies the theoretical treatment of coupled oscillator arrays. Lynch *et al.* [1.9] have shown that a narrowband coupling network decreases the

probability of array synchronization and reduces the oscillator's locking range.

The coupling phase $\Phi$ is the electrical length of the coupling transmission line. Choosing the proper coupling phase is critical for proper array operation since it plays a key role in determining the stable range of phase shifts and frequency distribution [1.2]. We wish to choose the coupling phase so as to maximize the mutual injection locking range. The in-phase synchronization of oscillators also depends on the coupling phase. Choosing an incorrect coupling phase can adversely affect the phase distribution and the mode of array operation. The coupling phase depends on the type of resonance exhibited by the oscillator. For in-phase synchronization, parallel resonant oscillators require a coupling phase which is an even integral multiple of $\pi$, whereas series resonant oscillators require a coupling phase which is an odd integral multiple of $\pi$ [1.2].

## B. Mutual Coupling

A transistor oscillator provides the flexibility of mutual coupling at different terminals. With a specific configuration, a transistor based oscillator presents either a series or a parallel resonant equivalent circuit at each terminal [1.8]. Fig. 1.2 shows an oscillator with a parallel resonant equivalent circuit, where *C* and *L* are the oscillator equivalent capacitance and inductance, $-G_D$ is the negative conductance exhibited by the active device, and $G_L$ is the load conductance.

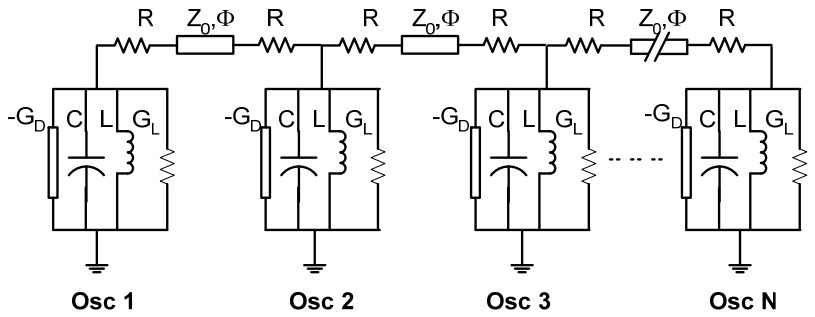

Fig. 1.2 Coupled oscillators with parallel resonant equivalent circuit.

Since only one distinct voltage can be defined, there is only one coupling configuration. For an array coupled with a linear, nearest neighbor coupling network (as shown in Fig. 1.1) and assuming weak coupling between the oscillators, the phase dynamic equation can be derived from [1.6] and is given as,

$$\begin{aligned}
\frac{\partial\theta_1}{\partial t} &= \omega_1 - \frac{\omega_1\kappa_0}{2Q}\sin\left(\theta_1 - \theta_2\right) \\
\frac{\partial\theta_i}{\partial t} &= \omega_i - \frac{\omega_i\kappa_0}{2Q}\left[\sin\left(\Phi + \theta_i - \theta_{i-1}\right) + \sin\left(\Phi + \theta_i - \theta_{i+1}\right)\right]. \qquad (1.2) \\
\frac{\partial\theta_N}{\partial t} &= \omega_N - \frac{\omega_N\kappa_0}{2Q}\sin\left(\theta_N - \theta_{N-1}\right)
\end{aligned}$$

A phase shift in the range of -90° to 90° is obtained by setting $\Phi = 0$ or $2n\pi$ .

An oscillator with a series resonant equivalent circuit provides multiple locations for coupling. Fig. 1.3 shows the different coupling configurations possible with a series resonant oscillator. C and L are the oscillator equivalent capacitance and inductance respectively, $-R_D$ is the negative resistance of the active device, and $R_L$ is the load resistance. For the case of coupling on resistors, assuming weak coupling between the oscillators, the phase dynamic equation for this coupling configuration is given as

$$\frac{\partial \theta_i}{\partial t} = \omega_i + \frac{{R_L}^2}{4LZ_0}\left[\sin\left(\Phi + \theta_i - \theta_{i-1}\right) + \sin\left(\Phi + \theta_i - \theta_{i+1}\right)\right]. \qquad (1.3)$$

An inter-element phase shift in the range of -90° to 90° is obtained by setting $\Phi = n\pi$, where *n* is odd. Using this, (1.3) simplifies to

$$\frac{\partial \theta_i}{\partial t} = \omega_i - \frac{{R_L}^2}{4LZ_0}\left[\sin\left(\theta_i - \theta_{i-1}\right) + \sin\left(\theta_i - \theta_{i+1}\right)\right]. \qquad (1.4)$$

For the case of coupling on inductors or capacitors, the phase dynamic equation reduces to

$$\frac{\partial \theta_i}{\partial t} = \omega_i + \frac{1}{4CZ_0}\left[\sin\left(\theta_{i-1} - \theta_i - \Phi\right) + \sin\left(\theta_{i+1} - \theta_i - \Phi\right)\right]. \qquad (1.5)$$

Once again, to obtain an inter-element phase shift in the range of -90° to 90°, we choose the coupling phase to be $\Phi = 0$ or $2\pi$. Coupling on an inductor or capacitor in a series resonant equivalent circuit produces a phase dynamic equation that is identical to that of a parallel resonant circuit. Thus, an oscillator operating at series resonance, when coupled on an inductor or a capacitor, requires a coupling phase which is an even integral multiple of $\pi$ [1.8]. In all, the location of coupling determines the coupling phase. Therefore, the coupling location must also be considered when determining the coupling phase required for in-phase synchronization of oscillator cells.

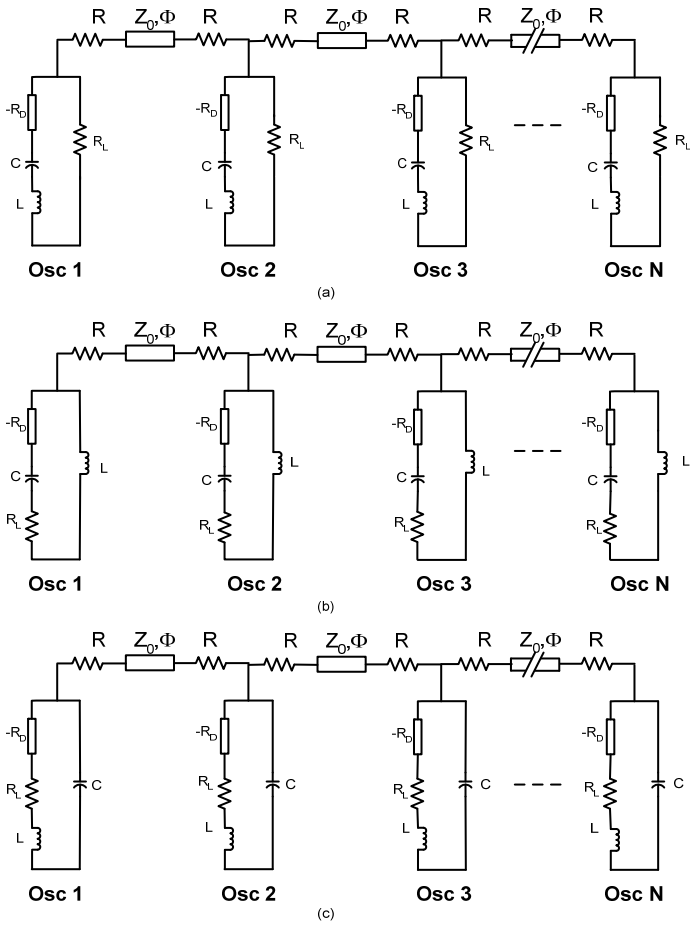


Fig. 1.3 Series resonant oscillators with coupling on (a) resistors (b) inductors (c) capacitors.

When the oscillator cells in a COA are coupled at the optimum coupling phase for in-phase synchronization with each other, the array radiates at broadside. The oscillator elements oscillate at equal amplitudes and the output power of the COA is concentrated in a single narrow beam and focused at broadside. Under such conditions the array is said to be operating in the desired mode. Nogi *et al.* [1.10] have shown that several modes are possible in a linear one-dimensional strongly coupled array and only one of these modes is desirable. The authors also provide a technique to suppress the undesired modes.

Chang *et al.* [1.2] have discussed the influence of the oscillator equivalent circuit on the stable modes. In their work they have investigated the ranges of stable phase shifts for different oscillator models and coupling phases.

When the oscillator cells are coupled with non-optimal coupling phase, the array operation degrades. With the array of oscillators each tuned to a common center frequency, and coupled with a coupling phase that is different from the ideal, the ensemble frequency deviates considerably from the individual oscillator's center frequency and the locking range will be less than expected. As a special case when the coupling phase is off by $\pi$ radians, the oscillators are out of phase with each other, the main beam is centered in the end-fire direction and the array may lock with a limited range.

## III. Oscillator Design and Experimental Results

The schematic of the open loop oscillator model used in this work is shown in Fig. 1.4. The voltage controlled oscillators (VCO's) use NEC 38018 HJFET devices as the negative resistance device and MA-COM 46580 varactor diodes for tuning. From Fig. 1.4, one can observe that the transistor terminals are associated with resonant circuits. In keeping with the interaction of the circuit resonances as described by Kurokawa [1.11], the resonant frequencies and the quality factors of these circuits can be adjusted to reduce the overall $Q$ of the oscillator. The interactions are complex and the presence of transmission lines further complicates the resonances and hence trial and error adjustments would be extremely inefficient.

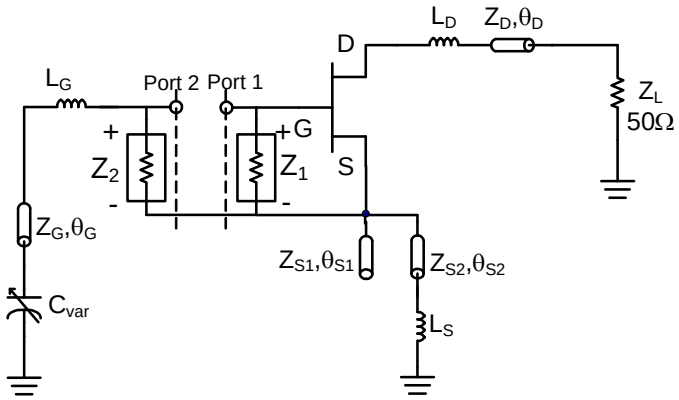

Fig. 1.4 Schematic of open loop oscillator model.

An optimization technique developed by Wang and Pearson is employed for the oscillator design [1.3].The resonant frequency of the oscillator design is 3.75 GHz. The goal of the design is to obtain a locking range of at least 375 MHz. Table 1.1 provides the circuit parameters optimized using Agilent ADS. The design uses small signal parameters of the transistor and varactor measured on a network analyzer. The oscillator layout is shown in Fig. 1.5. The transistor is biased at 1V, and with $R_S = 75\Omega$, this corresponds to a drain current of about 4mA. The predicted resonant properties of the oscillator are summarized in Table 1.2.

Table 1.1 Optimized oscillator parameters.

| Transmission Line | Length | Width | Lumped Element | |
|---|---|---|---|---|
| $TL_{D1}$ | 310 | 60 | $L_D$ | 2.2 nH |
| $TL_{S1}$ | 20 | 20 | $L_G$ | 1.2 nH |
| $TL_{S2}$ | 20 | 12 | $L_{RF\ BLOCK}$ | 47 nH |
| $TL_G$ | 136 | 12 | $R_S$ | 75 ohm |
| Output and Coupling Lines | | 25 | $C_{VAR}$ | 0.2-2.0 pF |
| | | | $R_{VAR}$ | 1 kOhm |
| $T_1$ | NEC 38018 | | $R_{C1}$ | 50 Ohm |
| | | | $R_{C2}$ | 50 Ohm |
| | | | $C_1$ | 47 pF |

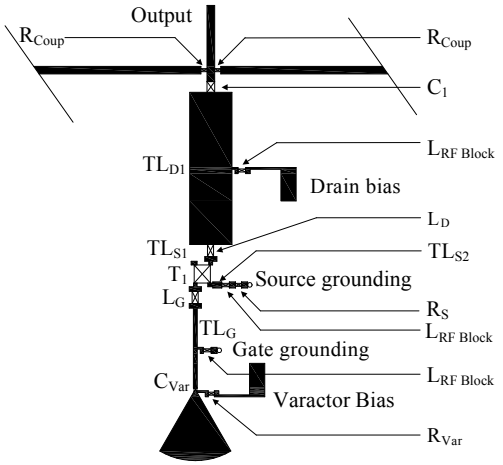

Fig. 1.5 Oscillator layout.

Table 1.2 Predicted oscillator resonant properties.

| Tuning Voltage (V) | Frequency (GHz) | Phase Slope (°/GHz) | Open Loop Gain (dB) | *Q* |
|---|---|---|---|---|
| 8 | 3.98 | 34.46 | 2.82 | 2.249 |
| 6 | 3.86 | 34.1 | 3.18 | 2.216 |
| 4 | 3.74 | 34.57 | 3.48 | 2.262 |
| 2 | 3.54 | 35.46 | 3.93 | 2.32 |

The objectives of the experiments were to elucidate the effects of coupling phase on the mutual injection locking range and the mode of array operation. To this end, we take advantage of the doubly resonant oscillator configuration, which offers the flexibility of mutual coupling at the drain and gate terminals with the drain terminal presenting a series resonance and the gate presenting a parallel resonance to the coupling network (see Fig. 1.4). Two three-element COAs were fabricated based on the optimized circuit parameters provided in Table 1.1 with coupling phases of $\Phi = \beta l = 2\pi, 3\pi$ and $4\pi$. The first array was mutually coupled at the drain while the second was coupled at the gate terminal. The circuits were fabricated on 0.635-mm thick Rogers TMM $10\left(\varepsilon_r = 9.2\right)$ board. The VCO's were coupled with 50-$\Omega$ transmission lines resistively loaded with chip resistors $R = Z_0$ (see Fig. 1.1 ).

The measurements on the arrays are performed in three stages. The first stage involves measuring the tuning characteristics of uncoupled individual oscillators. The output frequency and output power of each oscillator for every varactor bias is recorded. The second stage involved determining the mutual injection locking range (MILR) (as defined in (1.1)) exhibited by the two nearest neighboring elements. This stage proceeds as follows:

1. The coupling network between oscillators #1 and #2 is loaded by 50-$\Omega$ resistors. Oscillator #1 is switched on and centered at 3.75 GHz and the varactor bias voltage is recorded.
2. Oscillator #1 is switched off and oscillator #2 is switched on and centered at 3.75 GHz and the varactor bias voltage is recorded.

3. The oscillators are switched on simultaneously and the ensemble frequency is noted.
4. Oscillator #1 is then detuned lower in frequency until lock is broken. The frequency at which the lock is broken and the varactor bias are noted.
5. Oscillator #2 is switched off and the frequency that corresponds to the varactor bias of oscillator #1 is identified. Oscillator #1 is tuned back to 3.75 GHz.
6. Oscillator #2 is switched back on and oscillator #1 is detuned higher in frequency until lock is broken. Steps 4 and 5 are repeated to determine the mutual injection locking range of oscillator #1.
7. Steps 2-6 are repeated with the roles of the oscillators reversed and the locking range of oscillator #2 is determined.
8. Finally, oscillators #1 and #2 are uncoupled and oscillators #2 and #3 are coupled and the procedure is repeated to find the mutual injection locking ranges of oscillators #2 and #3.

The third stage involves determining the phase shift between the neighboring oscillator elements. This stage is performed in conjunction with the mutual injection locking measurements. A network analyzer is utilized for this purpose. Port 1 of the network analyzer is connected to the injection port at the center element and is set at a power level of at least 20 dB below the output power at injection point. 50-$\Omega$ terminations are connected at the injection ports of the other two oscillators. Port 2 of the network analyzer collects the output. Two neighboring oscillators are coupled and hence there are two outputs. Since we can measure only one output at a time, the other

oscillator is terminated with a 50-Ω load. The uncoupled oscillator is also terminated with a 50-Ω load.

A. Mutual Coupling at Drain and Gate Terminals

Fig. 1.6a and b show the photographs of the fabricated arrays with mutual coupling at the drain and gate terminals of the transistor respectively. Table 1.3 displays the injection locking ranges for all the coupled oscillator combinations. From Table 1.3, when the oscillators are mutually coupled at the drain, the highest injection locking ranges is recorded for the $3\pi$ coupling phase. When the coupling phase is $2\pi$ or $4\pi$ , the locking range is limited indicating that the coupling phase is non-optimal.

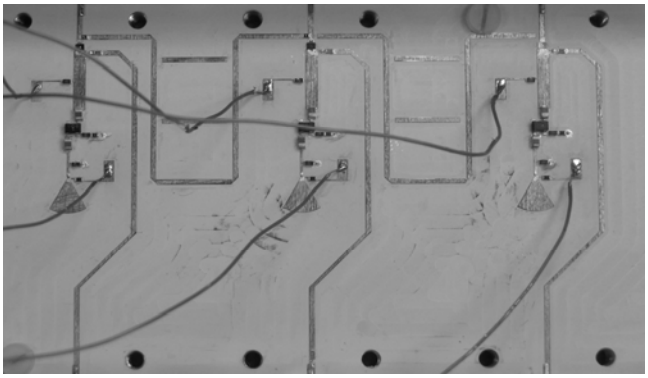

(a)

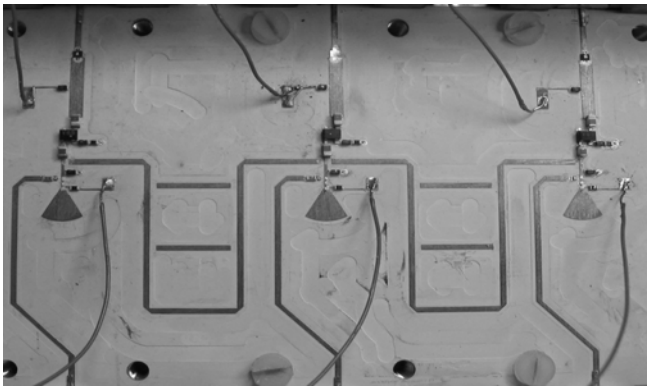

(b)

Fig. 1.6 Photograph of the three element COA (a) mutually coupled at the drain (b) mutually coupled at the gate. Coupling phase is changed irreversibly in the experiment by removing/connecting line sections in the 8-like shaped regions.

Table 1.3 MILR and ensemble frequency shift for all coupled oscillator combinations. Wider MILRs appear at the top.

| Coupling Location | Coupling Phase | Oscillators Coupled | Oscillator detuned | MILR (MHz) |
|---|---|---|---|---|
| Drain | 3π | 1 and 2 | 2 | 387 |
| | | | 1 | 381 |
| | | 2 and 3 | 2 | 370 |
| | | | 3 | 354 |
| Drain | 2π | 2 and 3 | 3 | 237 |
| | | | 2 | 233 |
| | | 1 and 2 | 1 | 220 |
| | | | 2 | 217 |
| Gate | 2π | 2 and 3 | 3 | 195 |
| | | | 2 | 179 |
| | | 1 and 2 | 2 | 187 |
| | | | 1 | 146 |
| Gate | 4π | 1 and 2 | 2 | 146 |
| | | | 1 | 126 |
| | | 2 and 3 | 3 | 109 |
| | | | 2 | 94 |
| Drain | 4π | 2 and 3 | 3 | 126 |
| | | | 2 | 109 |
| | | 1 and 2 | 1 | 94 |
| | | | 2 | 87 |
| Gate | 3π | 2 and 3 | 2 | 109 |
| | | | 3 | 109 |
| | | 1 and 2 | 2 | 109 |
| | | | 1 | 89 |

For mutual coupling at the gate, the largest mutual injection locking ranges is observed for the 2π coupling phase. The array performance with the 4π coupling phase is better than that with a 3π coupling phase, which yielded the least locking range. For both locations of mutual coupling the locking range obtained with a 2π coupling phase is greater than that with a 4π coupling phase. This is expected since the network with a 2π coupling phase is more broadband.

B. Mode of Array Operation for Each Coupling Location

Fig. 1.7-1.10 show the inter-element phase shift for each coupling network when the oscillators are mutually coupled at the drain and gate respectively. In phase synchronization of the oscillator elements occur for a coupling phase of $\Phi = 3\pi$ for mutual coupling at the drain and at $\Phi = 2\pi, 4\pi$ for mutual coupling at the gate. These choices of the coupling phase result in a broadside operation of the array, which is the desired mode of array operation. This shows that $\Phi = 3\pi$ is the optimal coupling phase for coupling at the drain whereas $\Phi = 2\pi, 4\pi$ is optimal for coupling at the gate.

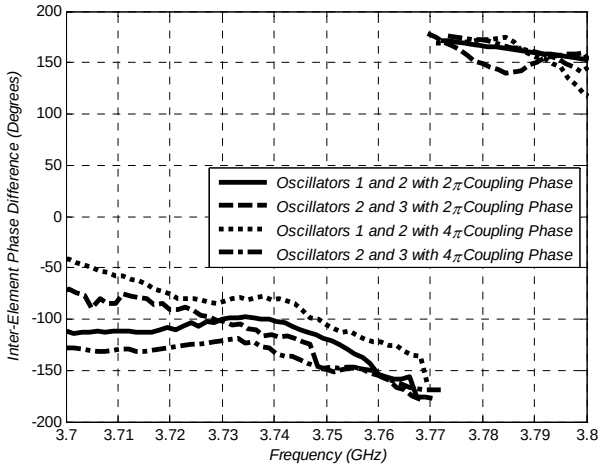


Fig. 1.7 Inter-element phase shift for 2π and 4π coupling phases for the array coupled at the drain.

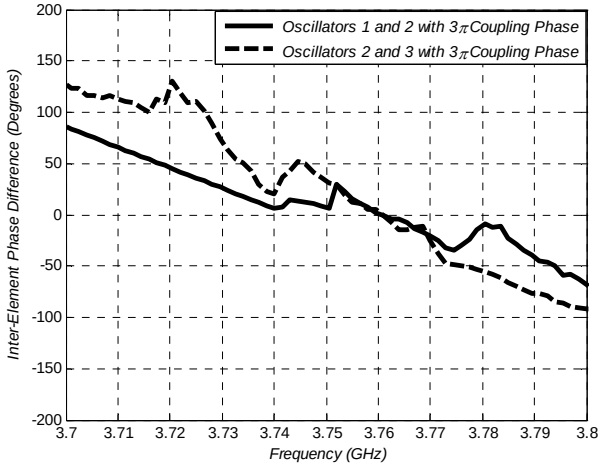


Fig. 1.8. Inter-element phase difference for the 3π coupling phase for the array coupled at the drain.

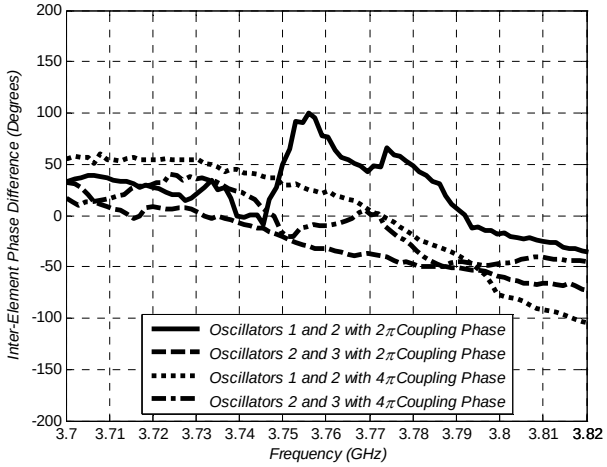


Fig. 1.9 Inter-element phase difference for the 2π and 4π coupling phases for the array coupled at the gate.

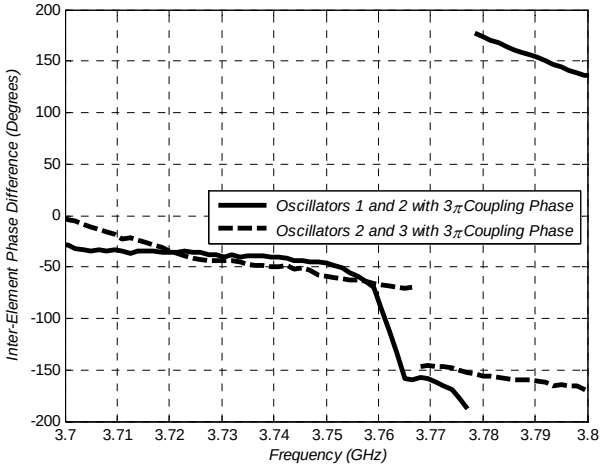


Fig. 1.10 Inter-element phase difference for the 3π coupling phase for the array coupled at the gate.

For both locations of coupling, when the coupling phase is off by $\Phi = 180^{\circ}$ from the optimum, the oscillators are out-of-phase with each other which causes the array to operate in the end-fire direction. Based on the measured results, one can conclude that a non-optimal coupling phase can result in out of phase synchronization which causes the array to operate in the end-fire direction and lowers the mutual injection locking range as well.

## IV. Conclusion

In this paper, the effect of coupling phase on the injection locking range and mode of array operation has been examined. A dually resonant oscillator configuration, which offered the flexibility of mutual coupling at different locations, was optimized for low *Q* and used to fabricate two three-element COAs - one in which oscillators were mutually coupled at the drain terminal and another in which oscillators were mutually coupled at the gate terminal. Broadside radiation of the array coupled at the drain occurred for a

coupling phase of 3π radians and yielded the largest MILR of 387 MHz. Out of phase synchronization of the oscillator elements occurred for coupling phases of 2π and 4π radians and resulted in reduced MILRs. For the array coupled at the gate, broadside radiation was obtained for coupling phases of 2π and 4π radians, whereas out of phase synchronization occured for coupling phase of 3π radians. Hence coupling with a non-optimal phase resulted in out of phase synchronization which significantly reduced the mutual injection locking ranges.

## Acknowledgment

The authors wish to gratefully acknowledge Jet Propulsion Lab for the support. We also acknowledge numerous fruitful technical conversations with Dr. Ronald J. Pogorzelski of Jet Propulsion Lab. We would like to thank the anonymous reviewers whose comments helped make this paper better.

## References

[1.1] R. J. Pogorzelski, "On the design of coupling networks for coupled oscillator arrays," *IEEE Trans. Antennas Propagat.,* vol. 51, pp. 794-801, April 2003.

[1.2] H. C. Chang, E. S. Shapiro, and R. A. York, "Influence of oscillator equivalent circuit on the stable modes of parallel-coupled oscillators," *IEEE Trans. Microwave Theory Tech.*, vol. 45, pp. 1232-1239, Aug. 1997.

[1.3] X. Wang and L. W. Pearson, "Design of coupled oscillator arrays without a posteriori tuning," *IEEE Trans. Microwave Theory Tech*., vol. 53, pp. 410-413, Jan. 2005.

[1.4] H. C. Chang, X. Cao, U. K. Mishra, and R. A. York, "Phase noise in externally injected oscillator arrays," *IEEE Trans. Microwave Theory Tech.*, vol. 45, pp. 2035-2042, Nov. 1997.

[1.5] C. Tompkins, V. Seetharam, and L. W. Pearson, "Improved mutual injection locking range for VCOs in a coupled oscillator system," *Proc. of IEEE Aerospace Conference*, March 2006.

[1.6] R. A. York, "Nonlinear analysis of phase relationships in quasi-optical oscillator arrays," *IEEE Trans. Microwave Theory Tech.*, vol. 41, pp. 1799-1809, October 1993.

[1.7] R. A. York, P. Liao, and J. J. Lynch, "Oscillator array dynamics with broadband N-port coupling network," *IEEE Trans. Microwave Theory Tech.*, vol. 42, pp. 2040-2045, Nov. 1994.

[1.8] J. Shen, "A study of the design of coupled oscillator phased arrays," Ph.D. dissertation, Dept. Elect. Comput. Eng., Clemson University, SC, 2002.

[1.9] J. J. Lynch and R. A. York, "Synchronization of oscillators through narrowband networks," *IEEE Trans. Microwave Theory Tech.*, vol. 49, pp. 237-249, Feb. 1994.

[1.10] S. Nogi, J. Lin, and T. Itoh, "Mode analysis and stabilization of a spatial power combining array with strongly coupled oscillators," *IEEE Trans. Microwave Theory Tech.*, vol. 41, pp. 1827-1837, Oct. 1993.

[1.11] K. Kurokawa, "Some basic characteristics of broadband negative resistance oscillator circuits," *Bell Systems Tech. Journal*, vol.48, pp. 1937-1955, Oct. 1971.

ANALYSIS OF STRONG COUPLING IN COUPLED OSCILLATOR ARRAYS

***Abstract*—Significant improvement in the mutual injection locking range (MILR) and phase noise can be obtained by strongly coupling the oscillator elements in a coupled oscillator array (COA). In this paper, the authors provide an analysis of the array properties in the strongly coupled regime. Previous analyses of COAs have employed a so-called broadband condition that substantially simplifies analysis. The broadband condition is observed to break down in the strongly coupled regime, a feature that is central in the understanding of the behavior of strongly coupled arrays. The observed improvement in the phase noise performance can be attributed to the highly resonant nature of the coupling network in the strongly coupled regime. The theory is verified using a five-element linear COA operating at 3.75 GHz. Significant improvements in the MILR and phase noise is reported. The beam steering capabilities of strongly coupled arrays are also presented.**

## I. Introduction

It is well known that sensitivity to component variation from cell-to-cell in a coupled oscillator array (COA) is problematic in array performance. This sensitivity is minimized if one employs wide-locking bandwidth oscillators. (In [2.1], a mutual injection locking range (MILR) parameter is introduced as an observable measure of locking bandwidth.) It has been shown that oscillator design can be optimized for wide-locking bandwidth by lowering the *Q* of the oscillators [2.2]. Operating on their own, low *Q* oscillators lead to poor phase noise performance in the array. However, this phase

noise can be controlled by injection locking the array to an external source that exhibits phase stability commensurate with the eventual application of the array.

The mutual injection locking range between two oscillators in an array is directly proportional to the coupling strength [2.3]. In the weakly coupled regime, the phase noise performance of the array improves with increase in the coupling strength. Thus strong coupling can possibly be utilized to widen the mutual injection locking range of the oscillators and improve the phase noise performance intrinsic to a given COA (prior to external injection locking). However, strong coupling between the elements complicates the analysis of array interaction. The amplitude variation along the array is negligible for the case of weak or loose coupling between the oscillator elements. This variation becomes significant for strongly coupled arrays. The coupling network becomes highly resonant at higher coupling strengths. For these reasons the analysis of strongly coupled oscillator arrays is not straightforward.

Strongly coupled arrays have been investigated by Nogi *et al.* [2.4]. They analyzed the issue of multiple modes in such arrays and showed that all but one of the resulting modes has amplitude variation across the array. They also present a technique to suppress the undesired modes. Lynch and York [2.5] investigated the effects of narrowband coupling networks on the synchronization properties of an array. They employed resistive coupling networks and performed analysis on weakly and strongly coupled oscillators for broadband and narrowband coupling. They concluded that narrowband coupling decreases the probability for the oscillators in an array to lock with each other.

In this paper an analysis of strongly coupled oscillator arrays is performed. The analysis focuses on obtaining a detailed understanding of the amplitude and phase distribution along the array for strongly coupled oscillators. Section II provides a brief introduction to COA theory. The oscillator array dynamics in the strongly coupled regime is presented. Section III provides the computed and the measured array amplitude and phase distributions. The measured mutual injection locking ranges are also presented in this section. The array amplitude variations result in undesired radiation patterns. Section IV is devoted to show a means of reducing the side lobe level by suitably attenuating the oscillator amplitudes. The beam steering capabilities of strongly coupled arrays are also evaluated. Section V discusses the phase noise characteristics of strongly coupled arrays. The phase noise theory developed by Chang *et al.* [2.6], [2.7] assuming weak coupling, is used to understand the effect of increased coupling strength on the phase noise performance of a COA. Then, the improvement in the phase noise performance of strongly coupled arrays is explained by computing the quality factor of the coupling network for various coupling strengths. The measured array free-running and injection locked phase noise characteristics are presented.

## II. Amplitude and Phase Dynamics

### A. Array dynamics assuming coupling network is broadband

Previous analysis of coupled oscillator arrays like that in Fig. 2.1 have demonstrated that the amplitude and phase of the individual oscillators can be expressed as [2.3], [2.8]:

$$\begin{aligned}\frac{\partial A_i}{\partial t} &= A_i.\mathrm{Im}\left\{F_i\left([A],[\theta]\right)\right\} \\ \frac{\partial \theta_i}{\partial t} &= \omega_i - \mathrm{Re}\left\{F_i\left([A],[\theta]\right)\right\}, \qquad i = 1,2,...N\end{aligned}, \tag{2.1}$$

where $A_i, \theta_i$ and $\omega_i$ are the amplitude, phase and free-running frequency of the $i^{\text{th}}$ oscillator respectively, and

$$F_i\left([A],[\theta]\right) = \frac{j\omega_i}{2Q}\left[\frac{\mu\left(1-\frac{A_i^2}{\alpha_i^2}\right) \pm \sum_{j=1}^{N}\frac{Y_{ij}}{G_L}\frac{A_j}{A_i}e^{j\left(-\Phi_{ij}+\theta_j-\theta_i\right)}}{1 \pm \frac{j\omega_i}{2Q}\sum_{j=1}^{N}\frac{1}{G_L}\frac{\partial Y_{ij}}{\partial \omega}\frac{A_j}{A_i}e^{j\left(-\Phi_{ij}+\theta_j-\theta_i\right)}}\right]. \tag{2.2}$$

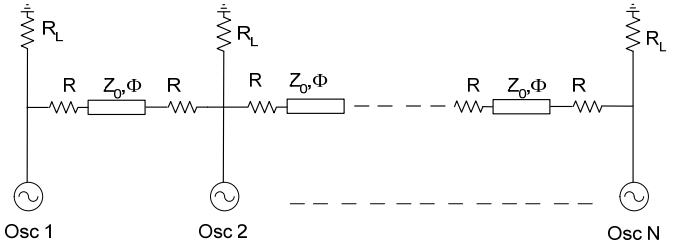


Fig. 2.1 An N-element coupled oscillator array.

The variables $A_i$ and $\theta_i$ comprise the elements of the vectors [A] and [$\theta$]. The parameters in (2.2) are $\mu$, the amplitude saturation factor; $\alpha_i$, the uncoupled amplitude of the $i^{\text{th}}$ oscillator; $Q$, oscillator quality factor; $G_L$, the load conductance; $\Phi_{ij}$ is the coupling phase between the $i^{\text{th}}$ and $j^{\text{th}}$ oscillators and $Y_{ij}$, the admittance of the coupling network from port $i$ to port $j$. Defining $\kappa_{ij} = \frac{Y_{ij}}{G_L}$ as the coupling coefficient, (2.2) can be simplified when the frequency dependence of the coupling network is much weaker than that of the oscillator, or

$$\left|\frac{\omega_i}{2Q}\sum_{j=1}^{N}\frac{\partial\kappa_{ij}}{\partial\omega}\frac{A_j}{A_i}\right| \ll 1, \tag{2.3}$$

and reduces (2.2) to

$$F_i\left([A],[\theta]\right)=\frac{j\omega_i}{2Q}\left[\mu\left(1-\frac{A_i^2}{\alpha_i^2}\right)\pm\sum_{j=1}^{N}\kappa_{ij}\frac{A_j}{A_i}e^{j\left(-\Phi_{ij}+\theta_j-\theta_i\right)}\right]. \tag{2.4}$$

Condition (2.3) is a broadband constraint which greatly simplifies the analysis of coupled oscillator arrays when it applies. The amplitude and phase dynamic equations can be derived from (2.1) and are given as:

$$\begin{aligned}\frac{dA_i}{dt}&=\frac{\omega_i A_i}{2Q}\left[\mu\left(1-\frac{A_i^2}{\alpha_i^2}\right)\pm\sum_{j=1}^{N}\kappa_{ij}\frac{A_j}{A_i}\cos\left(\Phi_{ij}+\theta_i-\theta_j\right)\right],\\ \frac{d\theta_i}{dt}&=\omega_i\mp\frac{\omega_i}{2Q}\sum_{j=1}^{N}\kappa_{ij}\frac{A_j}{A_i}\sin\left(\Phi_{ij}+\theta_i-\theta_j\right).\end{aligned} \tag{2.5}$$

In (2.2), (2.4) and (2.5) wherever $\pm$ sign is used, the upper sign applies to series resonant oscillators while the lower sign applies to parallel resonant oscillators. Equation (2.5) is valid provided the oscillator and the coupling network satisfy the condition [2.8],

$$\left|F_i\left([A],[\theta]\right)\right| \ll \omega_i. \tag{2.6}$$

Applying this to a typical bilateral, nearest neighbor coupling network (see Fig. 2.1) and setting $\Phi = n\pi$, where n=1, 2, 3…N, $\kappa_{ij}$ can be expressed as [2.8]:

$$\kappa_{ij} = \begin{cases} \dfrac{1}{2RG_L} = \kappa_0, & \text{if } i = j = 1 \text{ or } N \\ \dfrac{1}{RG_L} = 2\kappa_0, & \text{if } i = j \neq 1 \text{ or } N \\ \mp\dfrac{1}{2RG_L} e^{-\Phi_{ij}} = \mp\kappa_0 e^{-\Phi_{ij}}, & \text{if } |i - j| = 1 \\ 0, & \text{otherwise} \end{cases} \quad (2.7)$$

where $\kappa_0$ is the magnitude of the coupling coefficient and is termed the coupling strength. The coupling strength can be varied by changing the value of *R*.

The mutual injection locking range, which is defined as the maximum range by which the free-running frequencies of the oscillators can deviate collectively and still maintain a mutually locked state, is expressed as:

$$\Delta\omega_{lock} = \frac{\kappa_0 \omega_i}{2Q}. \quad (2.8)$$

From (2.8), a large $\kappa_0$ results in a wider mutual injection locking range. However, a large $\kappa_0$ causes an undesirable change in the array amplitudes [2.9] and presents a significant load to the oscillator [2.10]. Strong coupling ( $\kappa_0 > 0.5$ ) between the oscillator elements is desirable as long as other coupling features are not compromised.

For in-phase synchronization, series resonant oscillators require a coupling phase, $\Phi = n\pi$, where n is odd and parallel resonant oscillators require $\Phi = n\pi$, , where n is even [2.11]. In (2.5), the amplitude and phase dynamic equations using the broadband condition are given as:

$$\begin{aligned}\frac{dA_i}{dt} &= \frac{\omega_i A_i}{2Q}\left[\mu\left(1-\frac{A_i^2}{\alpha_i^2}\right)-\sum_{j=1}^{N}\kappa_{ij}\frac{A_j}{A_i}\cos\left(\theta_i-\theta_j\right)\right],\\ \frac{d\theta_i}{dt} &= \omega_i+\frac{\omega_i}{2Q}\sum_{j=1}^{N}\kappa_{ij}\frac{A_j}{A_i}\sin\left(\theta_i-\theta_j\right).\end{aligned} \tag{2.9}$$

Equation (2.9) is traditionally used to ascertain the amplitude and phase dynamics of COAs. These equations break down with large coupling factor, consistent with exceeding the limitations of the broadband condition.

B. Array dynamics assuming coupling network is not broadband

When the broadband condition (2.3) does not hold, a COA must be modeled with (2.2) including the resonant denominator term that the broadband condition obviates. This term bring the resonances of the coupling networks into play. Viz: assuming $R \neq Z_0$,

$$\frac{1}{G_L}\frac{\partial Y_{ij}}{\partial \omega}=\frac{\partial \kappa_{ij}}{\partial \omega}=\begin{cases}\dfrac{jn\pi\kappa_0\left(R^2-Z_o{}^2\right)}{2Z_0\omega_{oc}R}=jC_1, & if\ i\ =\ j=\ 1\ or\ N\\ \dfrac{jn\pi\kappa_0\left(R^2-Z_o{}^2\right)}{Z_0\omega_{oc}R}=j2C_1, & if\ i\ =\ j\neq\ 1\ or\ N\\ \dfrac{jn\pi\kappa_0\left(R^2+Z_o{}^2\right)}{2Z_0\omega_{oc}R}e^{-j\Phi_{ij}}=jC_2, & if\ \left|i-j\right|=\ 1\\ 0 \quad , & otherwise\end{cases} \tag{2.10}$$

where $\omega_{oc}$ is the resonant frequency of the coupling network.

The quality factor of the coupling network $Q_{net}$ is a useful parameter through which to view the networks' influence. $Q_{net}$ can be derived by applying the analogy of a resonant circuit [2.10]. Alternatively, $Q_{net}$ can also be obtained from (2.3) as:

$$Q_{net} = \pm \frac{j\omega_i}{2} \sum_{j=1}^{N} \frac{1}{G_L} \frac{\partial Y_{ij}}{\partial \omega} \frac{A_j}{A_i} e^{j\left(-\Phi_{ij}+\theta_j-\theta_i\right)}. \tag{2.11}$$

For in-phase synchronization of the oscillators, using (2.10), (2.11) simplifies as:

$$Q_{net}\Big|_{\omega_i=\omega_{oc}} = \frac{n\pi\kappa_0}{4RZ_0}\left[\left(R^2 - {Z_0}^2\right) + 2\cos\Delta\theta\left(R^2 + {Z_0}^2\right)\frac{A_j}{A_i}\right], \tag{2.12}$$

where $\Delta\theta = \theta_j - \theta_i$. Clearly, $Q_{net}$ is directly proportional to the coupling strength.

The L.H.S of (2.3) can be expressed as the magnitude of the ratio between the quality factors of the coupling network and the oscillator and is referred to as the broadband factor here. Table 2.1 shows the variation of $Q_{net}$ and the broadband factor with $\kappa_0$ for $Z_0 = 50\ \Omega$ and $\Delta\theta = 15^\circ$.

Table 2.1 Variation of $Q_{net}$ and the broadband factor with $\kappa_0$.

| R | $\kappa_0$ | $Q_{net}$ | $\left\lvert\frac{Q_{net}}{Q}\right\rvert$ |
|---|---|---|---|
| 100 | 0.25 | 1.24 | 0.06 |
| 50 | 0.5 | 1.52 | 0.08 |
| 25 | 1 | 2.62 | 0.13 |
| 16.67 | 1.5 | 4.45 | 0.22 |
| 12.5 | 2 | 8.03 | 0.4 |
| 10 | 2.5 | 10.34 | 0.517 |
| 5 | 5 | 41.11 | 2.056 |

The main purpose of the coupling resistor, *R* is to introduce loss and thereby reduce $Q_{net}$. This helps the coupling network to satisfy (2.3). The resistor also acts as a mode killer and suppresses the undesired modes that arise in a strongly coupled array [2.4]. From Table 2.1 one observes that as the value of resistor *R* is reduced to increase the coupling strength, $Q_{net}$ also increases. The lowered loading causes the coupling

network to become more highly resonant resulting in the breakdown of the broadband condition. From Table 2.1, one observes that (2.3) is clearly violated for $\kappa_0 \geq 1$.

The resonant nature of the coupling network complicates the interaction of strongly coupled oscillators. Therefore, (2.9) does not present an accurate representation of the amplitude and phase of the oscillator elements when the broadband condition is invalid. An accurate estimate of the behavior of the oscillator array under strong coupling conditions can be obtained by deriving the amplitude and phase dynamics equations without using (2.3).

Using (2.7), (2.12) in (2.2) and noting that for in-phase synchronization $\Phi = n\pi$, where $n$ is even for parallel resonant oscillators and odd for series resonant oscillators, the amplitude and phase dynamics equations can be derived from (2.1) as the following:

$$\frac{dA_1}{dt} = \frac{\omega_1 A_1}{2Q} \frac{\left[\begin{array}{l}\left(\mu\left(1-\frac{A_1^2}{\alpha_1^2}\right)-\kappa_0-\kappa_0\frac{A_2}{A_1}\cos\left(\theta_1-\theta_2\right)\right)\left(1+\frac{\omega_1}{2Q}\left(C_1+C_2\frac{A_2}{A_1}\cos\left(\theta_1-\theta_2\right)\right)\right)+ \\ \left(\frac{\omega_1}{2Q}\left(\kappa_0\frac{A_2}{A_1}\sin\left(\theta_1-\theta_2\right)\right)\left(C_2\frac{A_2}{A_1}\sin\left(\theta_1-\theta_2\right)\right)\right)\end{array}\right]}{\left(1+\frac{\omega_1}{2Q}\left(C_1+C_2\frac{A_2}{A_1}\cos\left(\theta_1-\theta_2\right)\right)\right)^2+\left(\frac{\omega_1}{2Q}C_2\frac{A_2}{A_1}\sin\left(\theta_1-\theta_2\right)\right)^2},$$

$$\frac{dA_i}{dt} = \frac{\omega_i A_i}{2Q} \frac{\left[\begin{array}{l}\left(\mu\left(1-\frac{A_i^2}{\alpha_i^2}\right)-2\kappa_0+\kappa_0\left(\begin{array}{l}\frac{A_{i-1}}{A_i}\cos\left(\theta_i-\theta_{i-1}\right)+ \\ \frac{A_{i+1}}{A_i}\cos\left(\theta_i-\theta_{i+1}\right)\end{array}\right)\right)\left(1+\frac{\omega_i}{2Q}\left(2C_1+C_2\left(\begin{array}{l}\frac{A_{i-1}}{A_i}\cos\left(\theta_i-\theta_{i-1}\right)+ \\ \frac{A_{i+1}}{A_i}\cos\left(\theta_i-\theta_{i+1}\right)\end{array}\right)\right)\right)- \\ \left(\frac{\omega_i}{2Q}\left(\kappa_0\left(\begin{array}{l}\frac{A_{i-1}}{A_i}\cos\left(\theta_i-\theta_{i-1}\right)+ \\ \frac{A_{i+1}}{A_i}\cos\left(\theta_i-\theta_{i+1}\right)\end{array}\right)\right)\left(C_2\left(\begin{array}{l}\frac{A_{i-1}}{A_i}\cos\left(\theta_i-\theta_{i-1}\right)+ \\ \frac{A_{i+1}}{A_i}\cos\left(\theta_i-\theta_{i+1}\right)\end{array}\right)\right)\right)\end{array}\right]}{\left(1+\frac{\omega_i}{2Q}\left(2C_1+C_2\left(\begin{array}{l}\frac{A_{i-1}}{A_i}\cos\left(\theta_i-\theta_{i-1}\right)+ \\ \frac{A_{i+1}}{A_i}\cos\left(\theta_i-\theta_{i+1}\right)\end{array}\right)\right)\right)^2+\left(\frac{\omega_i}{2Q}C_2\left(\begin{array}{l}\frac{A_{i-1}}{A_i}\cos\left(\theta_i-\theta_{i-1}\right)+ \\ \frac{A_{i+1}}{A_i}\cos\left(\theta_i-\theta_{i+1}\right)\end{array}\right)\right)^2},$$

$$\frac{dA_N}{dt}=\frac{\omega_N A_N}{2Q}\frac{\left[\begin{array}{l}\left(\mu\left(1-\frac{A_N^{\,2}}{\alpha_N^{\,2}}\right)-\kappa_0-\kappa_0\frac{A_{N-1}}{A_N}\cos\left(\theta_N-\theta_{N-1}\right)\right)\left(1+\frac{\omega_N}{2Q}\left(C_1+C_2\frac{A_{N-1}}{A_N}\cos\left(\theta_N-\theta_{N-1}\right)\right)\right)+\\ \left(\frac{\omega_N}{2Q}\left(\kappa_0\frac{A_{N-1}}{A_N}\sin\left(\theta_N-\theta_{N-1}\right)\right)\left(C_2\frac{A_{N-1}}{A_N}\sin\left(\theta_N-\theta_{N-1}\right)\right)\right)\end{array}\right]}{\left(1+\frac{\omega_N}{2Q}\left(C_1+C_2\frac{A_{N-1}}{A_N}\cos\left(\theta_N-\theta_{N-1}\right)\right)\right)^2+\left(\frac{\omega_N}{2Q}C_2\frac{A_{N-1}}{A_N}\sin\left(\theta_N-\theta_{N-1}\right)\right)^2},$$

(2.13a)

$$\frac{d\theta_1}{dt}=\omega_1+\frac{\omega_1}{2Q}\frac{\left[\begin{array}{l}\left(\mu\left(1-\frac{A_1^{\,2}}{\alpha_1^{\,2}}\right)-\kappa_0+\kappa_0\frac{A_2}{A_1}\cos\left(\theta_1-\theta_2\right)\right)\frac{\omega_1}{2Q}\left(\left(C_2\frac{A_2}{A_1}\sin\left(\theta_1-\theta_2\right)\right)\right)+\\ \left(1+\frac{\omega_1}{2Q}\left(C_1+C_2\frac{A_2}{A_1}\cos\left(\theta_1-\theta_2\right)\right)\right)\left(\left(\kappa_0\frac{A_2}{A_1}\sin\left(\theta_1-\theta_2\right)\right)\right)\end{array}\right]}{\left(1+\frac{\omega_1}{2Q}\left(C_1+C_2\frac{A_2}{A_1}\cos\left(\theta_1-\theta_2\right)\right)\right)^2+\left(\frac{\omega_1}{2Q}C_2\frac{A_2}{A_1}\sin\left(\theta_1-\theta_2\right)\right)^2},$$

$$\frac{d\theta_i}{dt}=\omega_i+\frac{\omega_i}{2Q}\frac{\left[\begin{array}{l}\left(\mu\left(1-\frac{A_i^{\,2}}{\alpha_i^{\,2}}\right)-2\kappa_0+\kappa_0\left(\begin{array}{l}\frac{A_{i-1}}{A_i}\cos\left(\theta_i-\theta_{i-1}\right)\\ +\frac{A_{i+1}}{A_i}\cos\left(\theta_i-\theta_{i+1}\right)\end{array}\right)\right)\frac{\omega_i C_2}{2Q}\left(\begin{array}{l}\frac{A_{i-1}}{A_i}\sin\left(\theta_i-\theta_{i-1}\right)+\\ \frac{A_{i+1}}{A_i}\sin\left(\theta_i-\theta_{i+1}\right)\end{array}\right)-\\ \left(1+\frac{\omega_i}{2Q}\left(2C_1+C_2\left(\begin{array}{l}\frac{A_{i-1}}{A_i}\cos\left(\theta_i-\theta_{i-1}\right)+\\ \frac{A_{i+1}}{A_i}\cos\left(\theta_i-\theta_{i+1}\right)\end{array}\right)\right)\right)\left(\kappa_0\left(\begin{array}{l}\frac{A_{i-1}}{A_i}\sin\left(\theta_i-\theta_{i-1}\right)+\\ \frac{A_{i+1}}{A_i}\sin\left(\theta_i-\theta_{i+1}\right)\end{array}\right)\right)\end{array}\right]}{\left(1+\frac{\omega_i}{2Q}\left(2C_1+C_2\left(\begin{array}{l}\frac{A_{i-1}}{A_i}\cos\left(\theta_i-\theta_{i-1}\right)+\\ \frac{A_{i+1}}{A_i}\cos\left(\theta_i-\theta_{i+1}\right)\end{array}\right)\right)\right)^2+\left(\frac{\omega_i C_2}{2Q}\left(\begin{array}{l}\frac{A_{i-1}}{A_i}\sin\left(\theta_i-\theta_{i-1}\right)+\\ \frac{A_{i+1}}{A_i}\sin\left(\theta_i-\theta_{i+1}\right)\end{array}\right)\right)^2},$$

$$\frac{d\theta_N}{dt}=\omega_N+\frac{\omega_N}{2Q}\frac{\left[\begin{array}{l}\left(\mu\left(1-\frac{A_N^{\,2}}{\alpha_N^{\,2}}\right)-\kappa_0+\kappa_0\frac{A_{N-1}}{A_N}\cos\left(\theta_N-\theta_{N-1}\right)\right)\frac{\omega_N}{2Q}\left(\left(C_2\frac{A_{N-1}}{A_N}\sin\left(\theta_N-\theta_{N-1}\right)\right)\right)+\\ \left(1+\frac{\omega_N}{2Q}\left(C_1+C_2\frac{A_{N-1}}{A_N}\cos\left(\theta_N-\theta_{N-1}\right)\right)\right)\left(\left(\kappa_0\frac{A_{N-1}}{A_N}\sin\left(\theta_N-\theta_{N-1}\right)\right)\right)\end{array}\right]}{\left(1+\frac{\omega_N}{2Q}\left(C_1+C_2\frac{A_{N-1}}{A_N}\cos\left(\theta_N-\theta_{N-1}\right)\right)\right)^2+\left(\frac{\omega_N}{2Q}\left(C_2\frac{A_{N-1}}{A_N}\sin\left(\theta_N-\theta_{N-1}\right)\right)\right)^2}.$$

(2.13b)

These equations are solved for a seven element array for an $15^\circ$ inter-element phase difference using a finite-difference approximation. In the simulation, the individual oscillators were characterized by $Q$ = 20 and $\mu = 2$. The free-running amplitudes are assumed to be 1. The resonant frequency of the oscillators was 3.75 GHz. The coupling

phase is $3\pi$ radians.

Fig. 2.2 and Fig. 2.3 show the variation of the array amplitude and phase with coupling strength respectively. We observe from Fig. 2.3 that the phase linearity sought in COAs persists even when the coupling is strong. However, we see that coupling influences the amplitude distribution across the array in a harmful way. Namely, the amplitudes of the oscillator elements grow toward the extremes of the array.

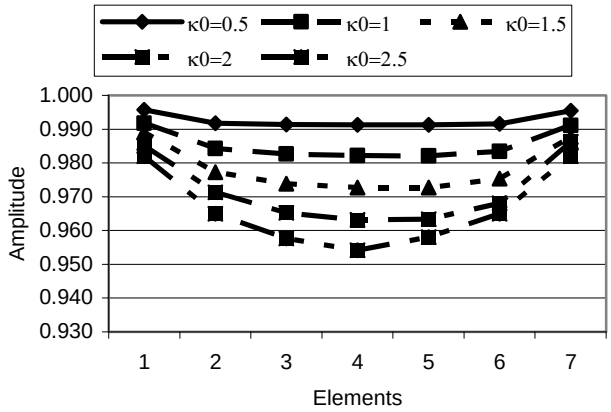


Fig. 2.2 Array amplitude variation with coupling strength for 15° inter-element phase difference without using broadband condition.

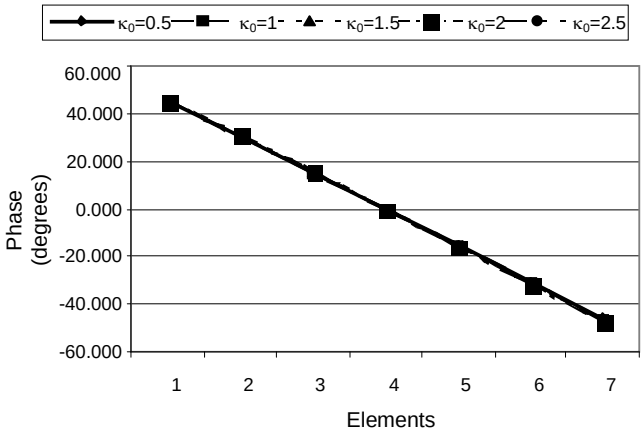


Fig. 2.3 Array phase variation with coupling strength for 15° inter-element phase difference without using broadband condition.

## III. Experimental Verification

The theoretical amplitude and phase distributions are verified on a five-element coupled oscillator array, which is built based on the oscillator cell design presented in [2.1]. The oscillators are coupled with 50-$\Omega$ transmission lines resistively loaded with chip resistors $R$ (see Fig. 2.1 ) and a coupling phase of $3\pi$ . The array was fabricated on 0.635-mm thick Rogers TMM 10 $\left(\varepsilon_r = 9.2\right)$ board.

The photograph of the array is shown in Fig. 2.4. Injection ports introduced at each element are utilized to measure the inter-element phase difference. The amplitude distribution across the array is measured for $10^\circ$, $20^\circ$ and $30^\circ$ inter-element phase differences using a network analyzer.

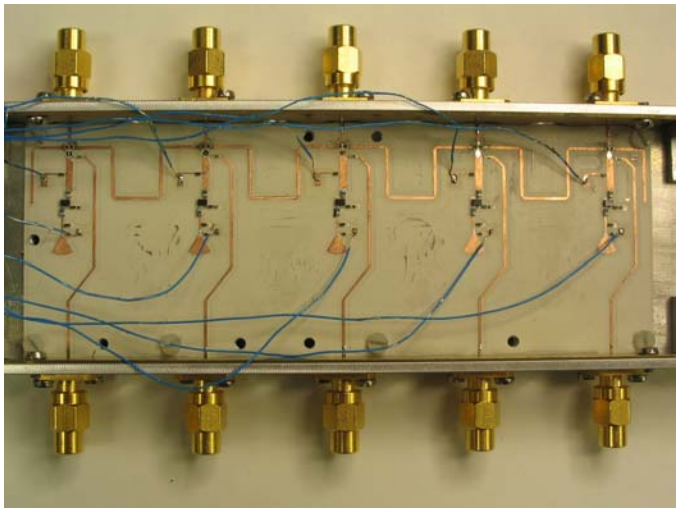

Fig. 2.4 Photograph of the five-element COA.

Fig. 2.5 shows the computed and measured array amplitude variation for various values of $\kappa_0$ for $20^\circ$ inter-element phase difference. The oscillator amplitudes for each $\kappa_0$ are normalized with respect to the measured amplitude of the center element.

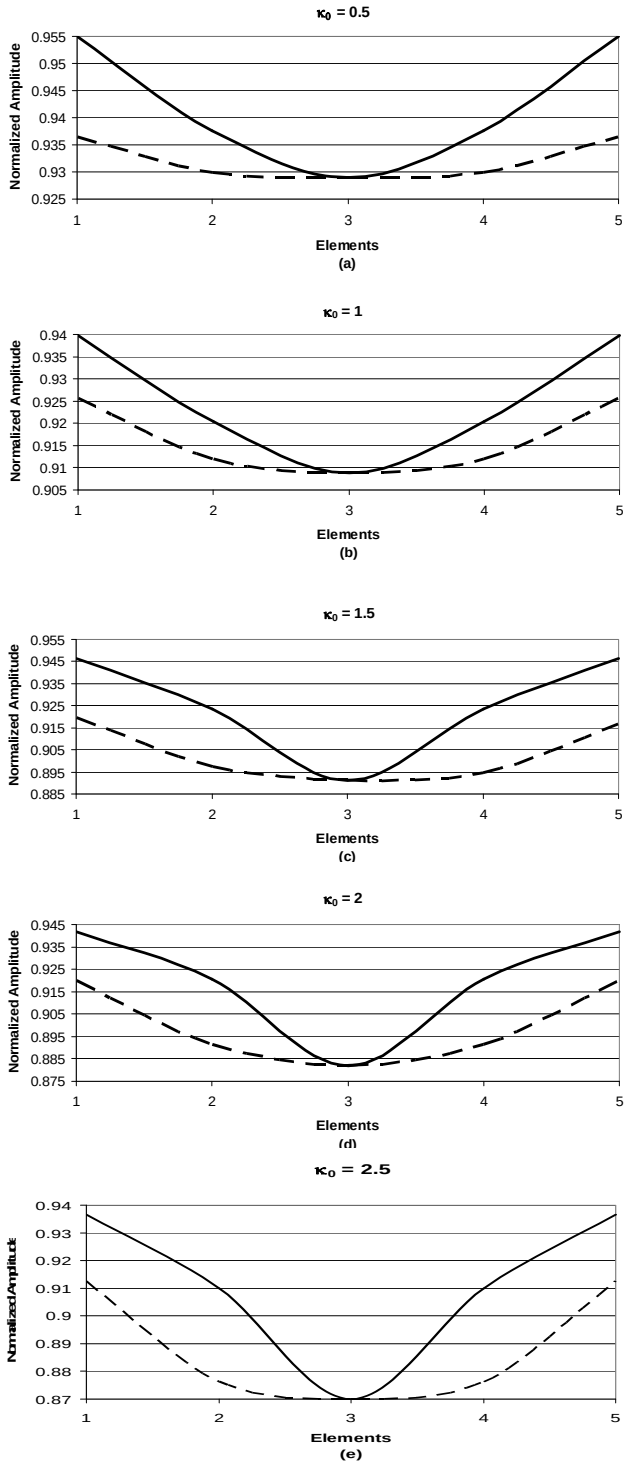


Fig. 2.5 Amplitude variation with $\kappa_0$ (a) $\kappa_0 = 0.5$ (b) $\kappa_0 = 1$ (c) $\kappa_0 = 1.5$ (d) $\kappa_0 = 2$ (e) $\kappa_0 = 2.5$. The solid and dashed lines represent measured and computed data respectively.

The computed and measured amplitudes are within a dB of each other. The mutual injection locking range exhibited by two nearest neighboring elements for various coupling strengths is determined by the procedure detailed in [2.1]. Table 2.2 presents the measured MILR exhibited by the oscillators for various coupling strengths.

Table 2.2 Mutual injection locking range exhibited by the oscillators for various coupling strengths.

| R | $\kappa_0$ | Oscillators coupled | Oscillator detuned | MILR | |
|---|---|---|---|---|---|
| | | | | MHz | ±% |
| 50 | 0.5 | 1 and 2 | 1 | 376 | 5.0 |
| | | | 2 | 420 | 5.6 |
| | | 2 and 3 | 2 | 354 | 4.7 |
| | | | 3 | 324 | 4.3 |
| | | 3 and 4 | 3 | 373 | 4.9 |
| | | | 4 | 365 | 4.8 |
| | | 4 and 5 | 4 | 309 | 4.1 |
| | | | 5 | 370 | 4.9 |
| 25 | 1 | 1 and 2 | 1 | 504 | 6.7 |
| | | | 2 | 567 | 7.5 |
| | | 2 and 3 | 2 | 462 | 6.1 |
| | | | 3 | 422 | 5.6 |
| | | 3 and 4 | 3 | 473 | 6.3 |
| | | | 4 | 473 | 6.3 |
| | | 4 and 5 | 4 | 428 | 5.7 |
| | | | 5 | 513 | 6.8 |
| 16 | 1.5 | 1 and 2 | 1 | 575 | 7.6 |
| | | | 2 | 641 | 8.5 |
| | | 2 and 3 | 2 | 543 | 7.2 |
| | | | 3 | 536 | 7.1 |
| | | 3 and 4 | 3 | 585 | 7.8 |
| | | | 4 | 589 | 7.8 |
| | | 4 and 5 | 4 | 569 | 7.6 |
| | | | 5 | 666 | 8.9 |
| 13 | 2 | 1 and 2 | 1 | 607 | 8.1 |
| | | | 2 | 683 | 9.1 |
| | | 2 and 3 | 2 | 657 | 8.7 |
| | | | 3 | 658 | 8.8 |
| | | 3 and 4 | 3 | 680 | 9.0 |
| | | | 4 | 687 | 9.1 |
| | | 4 and 5 | 4 | 620 | 8.2 |
| | | | 5 | 726 | 9.6 |
| 10 | 2.5 | 1 and 2 | 1 | 636 | 8.5 |
| | | | 2 | 707 | 9.4 |
| | | 2 and 3 | 2 | 679 | 9.0 |
| | | | 3 | 673 | 9.0 |
| | | 3 and 4 | 3 | 703 | 9.4 |
| | | | 4 | 710 | 9.5 |
| | | 4 and 5 | 4 | 658 | 8.8 |
| | | | 5 | 743 | 9.9 |

One observes that the MILR increases with the coupling strength. For $\kappa_0 = 2.5$, the MILR exhibited by oscillator #5 is about 750 MHz or $\pm 10\%$ of 3.75 GHz. To the authors' knowledge, this is the largest MILR reported in literature to date.

## IV. Radiation Patterns and Beam Steering

The amplitude variations exhibited in Fig. 2.5 result in poor radiation patterns. Since the end oscillators have greater amplitudes than the interior oscillators, when such an array is employed in a phased array system, the side lobe level is undesirably large. A better radiation pattern can be obtained by introducing an amplitude taper wherein the end oscillator elements have the lowest amplitude in the array. In our experimental work, this is accomplished by amplifying each VCO output with a Mini-Circuits ERA-1SM+ buffer amplifier and coaxial attenuators were used to trim the output power. Phase relationships were maintained by using equal numbers of attenuators in all paths. In practice, one might employ amplifiers with trimmable gain so that efficiency is maintained. The trimmed power levels are delivered to a patch antenna, 17.8mm wide and 12.5mm long, which employed a quarter wave transformer matching section to present a 50-$\Omega$ load to the oscillator. The antenna spacing is 29.5mm which is about $0.4\,\lambda_0$ at the oscillation frequency. The buffer amplifier and patch elements are realized on a separate Rogers TMM 10 board. Fig. 2.6 shows the photograph of the oscillator array connected to the patch antennas.

Fig. 2.6 Photograph of the oscillator elements connected to the patch antennas. Oscillator cells, with amplifiers reside in the box below. Attenuators of chosen value connect the outputs of the cells to the patches through flexible cables.

Fig. 2.7-2.11 show the measured array broadside and steered radiation patterns for various $\kappa_0$ before and the after application of the amplitude taper.

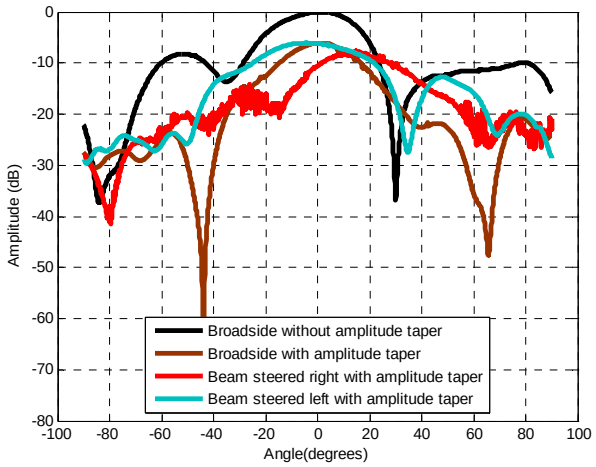


Fig. 2.7 Radiation patterns before and after amplitude tapering for $\kappa_0 = 0.5$.

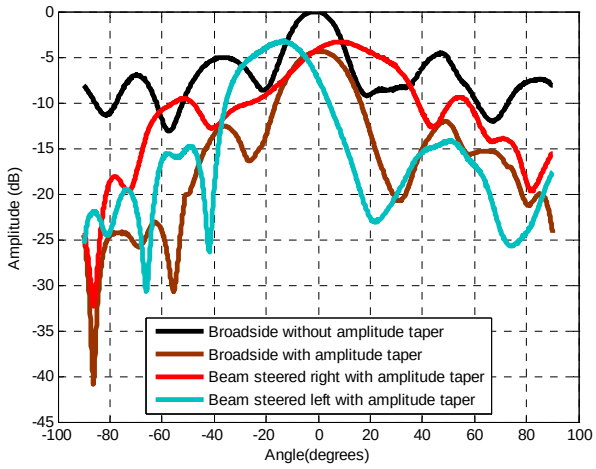


Fig. 2.8 Radiation patterns before and after amplitude tapering for $\kappa_0 = 1$.

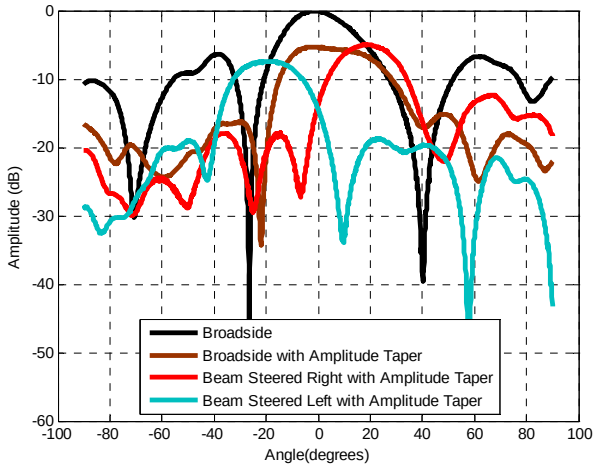


Fig. 2.9 Radiation patterns before and after amplitude tapering for $\kappa_0 = 1.5$.

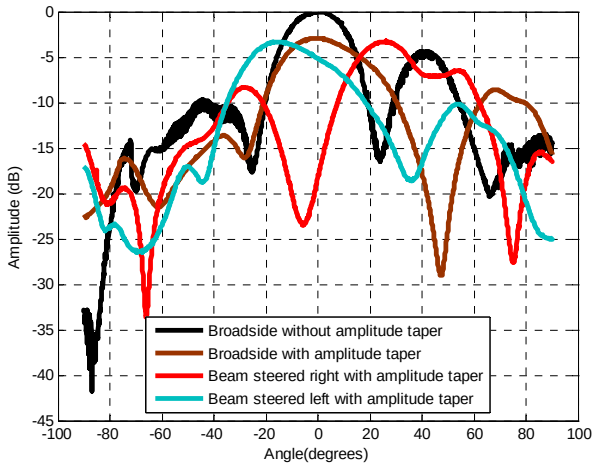


Fig. 2.10 Radiation patterns before and after amplitude tapering for $\kappa_0$=2.

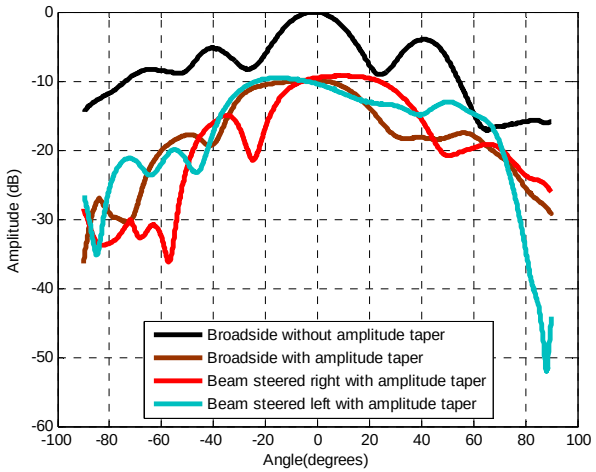


Fig. 2.11 Radiation patterns before and after amplitude tapering for $\kappa_0$=2.5.

Table 2.3 displays the radiated amplitudes with and without the taper. Table 2.4 shows the maximum beam steering from broadside exhibited by the COA for different coupling strengths. The beam steering is limited by the mutual injection locking range. It is noteworthy that for $\kappa_0$=2.5 the MILR limit was not encountered. The tuning range of

the end oscillators (#1 and #5) was saturated before lock was broken. Consequently, the last numbers in Table 2.4 do not relate monotonically to the remainder of the table.

Table 2.3 Measured amplitudes with and without amplitude taper. The amplitudes are measured at a distance of 2.67 m from the radiating patches.

| $\kappa_0$ | Oscillator # | Relative amplitudes without taper (dBm) | Relative amplitudes with taper (dBm) |
|---|---|---|---|
| 0.5 | 1 | -2 | -22 |
| | 2 | -4 | -7 |
| | 3 | -5 | -9 |
| | 4 | -5 | -5 |
| | 5 | 0 | -17 |
| 1 | 1 | -2 | -12 |
| | 2 | -6 | -7 |
| | 3 | -6 | -7 |
| | 4 | -3 | -4 |
| | 5 | 0 | -8 |
| 1.5 | 1 | -3 | -11 |
| | 2 | -7 | -8 |
| | 3 | -5 | -6 |
| | 4 | -3 | -5 |
| | 5 | 0 | -8 |
| 2 | 1 | -2 | -13 |
| | 2 | -8 | -9 |
| | 3 | -8 | -9 |
| | 4 | -6 | -8 |
| | 5 | 0 | -11 |
| 2.5 | 1 | -2 | -15 |
| | 2 | -6 | -7 |
| | 3 | -8 | -8 |
| | 4 | -4 | -6 |
| | 5 | 0 | -11 |

Table 2.4 Measured beam steering off broadside for various $\kappa_0$.

| $\kappa_0$ | Measured beam steering from broadside |
|---|---|
| 0.5 | +12.9/-6.1 |
| 1 | +8.6/-13.8 |
| 1.5 | +20.2/-19.2 |
| 2 | +27.3/-14.6 |
| 2.5 | +10.6/-14.2 |

## V. Phase Noise Characteristics of Strongly Coupled Oscillator Arrays

Assuming weak coupling between the oscillator elements the phase noise of an $N$ element COA injection locked to an external source is given by [2.7]:

$$\left|\delta\theta_{total}\right| = \frac{\left|B_n\right|^2}{N^2}\sum_{j=1}^{N}\left|\sum_{i=1}^{N} p_{ij}\right|^2 + \frac{\left|\delta\psi_{inj}\right|^2}{N^2}\sum_{j=1}^{N}\left|\sum_{i=1}^{N} p_{ij}\rho'_j\right|^2 \tag{2.14}$$

where $\left|\tilde{B}_n\right|^2$ is the power spectral density of the oscillator's quadrate noise source, $\left|\delta\psi_{inj}\right|^2$ is the phase noise of the external source, $\rho'_j$ is a vector of the relative strengths of the injection signals and $p_{ij}$ is a matrix representing the coupling topology. For the free running COA, the second term on the right hand side of (2.14) becomes zero. The elements $p_{ij}$ for the free running and injected arrays are computed from the inverse of matrix $\overline{\overline{N}}$ given in (2.15) and (2.16) respectively [2.6], [2.7]

$$\overline{\overline{N}} = y\begin{bmatrix} -1-jx & 1 & 0 & 0 & \cdots & 0 \\ 1 & -2-jx & 1 & 0 & \cdots & 0 \\ 0 & 1 & -2-jx & 1 & \ddots & \vdots \\ \vdots & \ddots & \ddots & \ddots & \ddots & 0 \\ 0 & \cdots & \ddots & 1 & -2-jx & 1 \\ 0 & 0 & \cdots & 0 & 1 & -1-jx \end{bmatrix}, \tag{2.15}$$

where $x = \dfrac{\omega\kappa_0}{\Delta\omega_{lock}\cos\Delta\hat{\theta}}$ and $y = \kappa_0\cos\Delta\hat{\theta}$,

$$\overline{\overline{N}} = \begin{bmatrix} z - jx - y & y & 0 & \cdots & 0 \\ y & z - jx - y & y & \ddots & \vdots \\ 0 & y & \ddots & y & 0 \\ \vdots & \ddots & y & z - jx - 2y & y \\ 0 & \cdots & 0 & y & z - jx - y \end{bmatrix}, \tag{2.16}$$

where $z = \rho_i'$.

Using (2.15) and (2.16) in (2.14) it is clear that within the weakly coupled regime, the phase noise performance of a COA improves as $\kappa_0$ increases. Analysis of the phase noise of strongly coupled arrays on similar lines is extremely complicated due to the resonant nature of the coupling network. However the phase noise performance of strongly coupled oscillator arrays can be understood by observing $Q_{net}$ .The increase in $Q_{net}$ with $\kappa_0$ (see Table 2.1) can be interpreted as an increase in the overall *Q* of the COA system, which results in the improvement in the phase noise performance of the COA.

The phase noise characteristics of the five-element COA is measured using an Aeroflex PN9000B phase noise measurement system. An Agilent E4433B, ESG-D signal generator is used as the external injection source. The oscillators' output power was -10 dBm, and for injection signal strength of -45 dBm, the injection ratio is calculated as $\rho = P_{inj} + P_{loss} - P_{osc}$ = -45dBm. $P_{loss}$ is the loss associated with the cables and the injection port.

Fig. 2.12 and Fig. 2.13 show the measured phase noise characteristics of the free running and injected array respectively for different values of $\kappa_0$ in the strongly coupled

regime. It is clear from Fig. 2.12 and Fig. 2.13 that the phase noise performance of the array improves with increase in $\kappa_0$. A 25 dB improvement in the free running array phase noise is observed on increasing $\kappa_0$ from 0.5 to 2.5. Moreover, a higher $\kappa_0$ causes the injected array to operate closer to the noise floor. Hence, strongly coupled oscillator arrays can operate almost at the noise floor with less injection signal power than weakly coupled arrays.

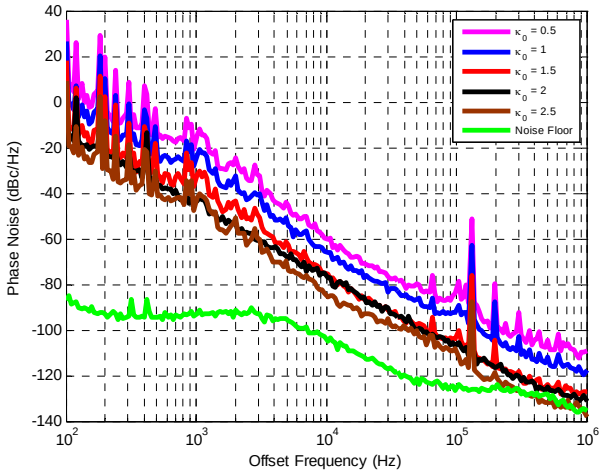


Fig. 2.12 Variation of array free running phase noise with $\kappa_0$.

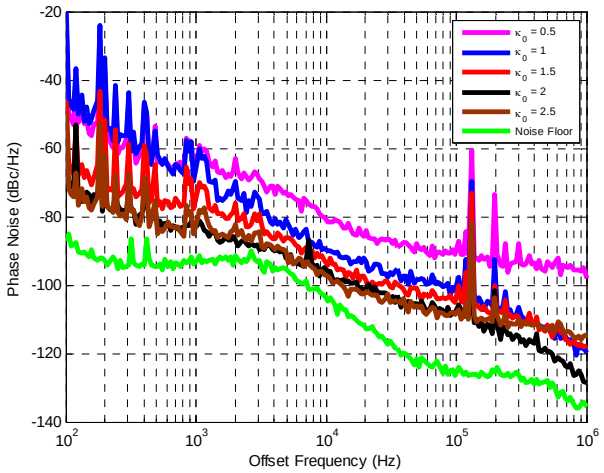


Fig. 2.13 Variation of array phase noise with $\kappa_0$ for $\rho$ =-45 dBm.

## VI. Conclusion

In this paper, the behavior of coupled oscillator arrays in the strongly coupled regime was analyzed. For large coupling strengths, the resonant nature of the coupling network increases resulting in the breakdown of the broadband condition. A five-element array operating at 10 GHz was fabricated and the mutual injection locking range, array phase noise and beam steering characteristics were evaluated for coupling strengths varying from 0.5 to 2.5. A two fold improvement in the mutual injection locking range was observed. At an offset of 10 kHz from the carrier a 25 dB improvement in the array free-running phase noise performance was shown. Injection locked strongly coupled arrays were shown to operate closer to the noise floor with less injection signal power than weakly coupled arrays. Therefore, strong coupling offers simultaneous improvement of the mutual injection locking range and the array phase noise. This is important since usually the improvement in the phase noise performance is usually obtained at the

expense of mutual injection locking range and vice versa. Tapering of the array amplitude distribution was utilized to achieve reduction in the side lobe level at the expense of beam directivity and effective isotropic radiated power.

## References


[2.1] V. Seetharam, J. Shen and L. W. Pearson, "Effect of coupling phase on mutual injection locking range in coupled oscillator arrays," *IEEE Trans. Antennas Propagat.,* under review.

[2.2] X. Wang and L. W. Pearson, "Design of coupled- oscillator arrays without a posteriori tuning," *IEEE Trans. Microwave Theory Tech.*, vol. 53, pp. 410-413, Jan. 2005.

[2.3] R. A. York, "Nonlinear analysis of phase relationships in quasi-optical oscillator arrays," *IEEE Trans. Microwave Theory Tech.*, vol. 41, pp. 1799-1807, Oct. 1993.

[2.4] S. Nogi, J. Lin, and T. Itoh, "Mode analysis and stabilization of a spatial power combining array with strongly coupled oscillators," *IEEE Trans. Microwave Theory Tech.*, vol. 41, pp. 1827-1837, Oct. 1993.

[2.5] J. J. Lynch and R. A. York, "Synchronization of oscillators coupled through narrow-band networks," *IEEE Trans. Microwave Theory Tech.*, vol. 49, pp. 237-249, Feb. 2001.

[2.6] H. C. Chang, X. Cao, U. K. Mishra, and R. A. York, "Phase noise in coupled oscillators: theory and experiment," *IEEE Trans. Microwave Theory Tech.*, vol. 45, pp. 604-615, May 1997.

[2.7] H. C. Chang, X. Cao, M. J. Vaughan, U. K. Mishra, and R.A. York, "Phase noise in externally injection-locked oscillator arrays," *IEEE Trans. Microwave Theory Tech.*, vol. 45, pp. 2035-2042, Nov. 1997.

[2.8] R. A. York, P. Liao, and J. J. Lynch, "Oscillator array dynamics with broadband N-Port coupling networks," *IEEE Trans. Microwave Theory Tech.*, vol. 42, pp. 2040-2045, Nov. 1994.

[2.9] Jinjin Shen, "A study of the design of coupled oscillator phased arrays," Ph.D. dissertation, Dept. Elec. Comp. Engr., Clemson University, SC, 2002.

[2.10] R. J. Pogorzelski, "On the design of coupling networks for coupled oscillator arrays," *IEEE Trans. Antennas Propagat.,* vol. 51, pp. 794-801, April 2003.

[2.11] H. C. Chang, E. S. Shapiro, R. A. York, " Influence of the oscillator equivalent circuit on the stable modes of parallel-coupled oscillators," *IEEE Trans. Microwave Theory Tech.*, vol. 45, pp 1232-1239, Aug. 1997.

MULTIPORT INJECTION LOCKING FOR IMPROVED BEAM STEERING AND PHASE NOISE IN COUPLED OSCILLATOR ARRAYS

**Abstract— In this paper, the authors extend earlier work on the use of multiport injection locking technique for simultaneous improvement in array beam steering and phase noise performances. Simultaneous injection locking of multiple oscillators in a COA with appropriate phase shift provides a convenient way to set the required inter-element phase shift thereby controlling the beam steering. A nine-element COA at 10 GHz is used to demonstrate the beam steering capability and phase noise performance using this technique. The best beam steering and phase noise performance is obtained for the case when the elements close to the center element are chosen for injection locking. The measured beam steering and phase noise data is compared with the theoretical results.**

## I. Introduction

Coupled oscillator arrays (COAs) possess synchronization properties that make them attractive for beam steering applications. Linear phase progression along the array can be obtained by anti-symmetric frequency detuning of the end elements in a linear array or the edge elements in a two-dimensional array [3.1] –i.e., tuning the free-running frequencies of the elements on opposite edges above and below the ensemble frequency of the coupled oscillation. Using this method, Liao *et al.* [3.2] and Pogorzelski *et al.* [3.3] achieve 54% and 43% of the theoretical scanning range respectively. The main beam can also be steered off broadside by simultaneous injection locking of multiple oscillator

elements with appropriate phase shifts from a single injection source. Stephan [3.4], [3.5] proposed beam-scanning by locking the first and last oscillators in a linear array by means of two injection signals with a prescribed phase difference. This scheme requires higher injection signal power to force the output phases of the array. The injection locking locations determine the phase progression and hence the beam steering. Additional beam steering can be obtained by employing frequency detuning with the multiport injection locking technique.

Tompkins [3.6] created an $180^{\circ}$ phase difference between the end elements without anti-symmetric frequency tuning of the end elements. An $180^{\circ}$ hybrid coupler is used to divide the signal from a single external injection source and the divided signals are fed to the end oscillators in a nine-element COA. Using this scheme, the main lobe is steered $6.5^{\circ}$ from broadside.

Injection locking is critical to practical deployment of COAs. Low *Q* oscillators constitute the best elements for a COA. Their wide locking range properties allow COAs to cohere well and minimize sensitivity to component variation [3.1]. However, the phase noise characteristics of free-running low-Q oscillators are quite poor. High quality phase noise performance (say -120 dBc/Hz at 10 kHz offset) is necessary for military compact radar applications and commercial digital communication systems. Low phase noise results in small bit error rates (BER), which is critical for high-fidelity transmission. In Doppler radar, low phase noise is necessary for resolution of stationary and near-stationary objects. The injection of a COA with a low-phase-noise reference signal can lock the array at a noise level commensurate with the injection source. Chang, *et al.*,

demonstrate that the injection of a COA with a low-phase-noise reference signal can lock the array at a commensurately low phase-noise level [3.7].

Chang *et al.* [3.8] analyzed the phase noise of a mutually synchronized oscillator system neglecting the amplitude noise, and amplitude modulation to phase modulation conversion. They showed that in a well-designed array, the near-carrier phase noise of an N element array improved by factor of $\frac{1}{N}$ over the individual oscillator's phase noise. The injection locking location is influential in the phase noise characteristics of an array. In a linear array, if only one port is used for injection locking, the greatest improvement in phase noise (compared to free running array) is observed when the array is injection locked at the center element [3.7]. This maximizes the influence of the injected signal power on elements farthest away from the injection point. When the array is injection locked at the other elements, less improvement over the free running array phase noise is observed due to unequal distribution of injected power among the elements. For small arrays injection locking at one port may be sufficient, but phase noise improvement diminishes for larger arrays [3.7].

For large arrays, it has been shown that injection locking at multiple oscillators in the array provides an added improvement in the phase noise [3.6]. In this work, the authors have extended the theory developed by [3.7] to include multiport injection locking. Chang *et al.* [3.7] assume unilateral injection locking, which does not consider the reverse coupling from the array to the external injection source. Such a reverse coupling is observed by [3.6] and this phenomenon was referred to as non-reciprocal bi-directional injection locking (NBIL). The theory developed by [3.7], [3.8] is extended to

account for NBIL. The authors of [3.6] employ one, two and three port injection locking of a nine element coupled oscillator array using oscillator cells designed to operate at 10 GHz. They show that, for particular injection signal strength, two and three port injection locking of the array provide a 10 and 15 dB improvement in phase noise respectively over single port injection locking.

With multiport injection, one must provide a number of injection signals with proper phase relationship to one another. This is similar to the operation of a phased array, of course, except that far fewer signals must be provided. One can think of a COA with multiport injection as having phases set by injection at selected elements, with the oscillator dynamics providing a phase interpolation between injected oscillator elements. Another point of view is to think of the aggregate of the oscillator cells between injected oscillators as electronically interpolating sub-arrays.

In this paper, multiport injection locking is explored for enhancement of beam steering capabilities and phase noise performance of a nine element COA using oscillator cells operating at 10 GHz. Section II is devoted to show the considerable improvement in the beam steering capabilities of the array by employing injection locking at multiple oscillators. The far field patterns are measured when an $180^{\circ}$ phase difference is shared between different oscillator combinations. Frequency detuning of the end oscillators for the different multiport injection locking scenarios is performed to show that additional beam steering can be achieved by employing the two methods simultaneously. Section III is devoted to show the additional improvement in phase noise than reported by [3.6]. A considerable improvement in the phase noise of the array is shown by choosing the

inner oscillators (oscillators other than the end elements) as the locations for multiport injection locking. To this end, two, three and four port injection locking was performed. The array was fabricated with ports on each oscillator allowing injection locking with external sources. The NBIL phenomenon was taken into consideration and the measured data was compared with the theoretical results.

## II. Use of Multiport Injection Locking for Enhancement of Array Beam Steering Capability

### A. Principle and Motivation

Phase progression along a COA can be easily achieved by frequency detuning the first and last oscillators in a linear array or the edge oscillators in a two-dimensional array [3.1]. Using this scheme, the maximum achievable beam steering is limited by the stable phase shifts allowed. Linear phase progression along a COA can also be obtained by simultaneous injection locking of multiple oscillator elements with an appropriate phase shift. Stephan [3.4] achieved beam-scanning by simultaneously injection locking the end oscillators in a linear array with two injection signals with a prescribed phase difference. Ideally this phase difference is then equally divided along the chain resulting in a linear phase progression along the array. Thus the inter-element phase shift depends on the number of oscillators in the array and hence for large arrays, only small phase shifts can be obtained, which limits the beam steering.

For larger arrays, greater phase shifts can be obtained by simultaneous injection locking of the inner oscillators with an appropriate phase difference from a single injection source. Since the number of elements sharing this phase difference is reduced,

greater phase shifts are possible. The injection locking locations determine the inter-element phase shift and hence the beam steering. This allows one to control the beam steering by adjusting the phase shift between the oscillator elements. Thus by moving the injection locking locations closer to the center oscillator, the beam-scanning capability of the array is enhanced. However this technique requires higher injection locking powers than the frequency detuning scheme to force the output phases of the array.

B. Oscillator Schematic and Fabrication

A nine-element COA is utilized to verify the beam steering capabilities of the multiport injection locking scheme. The schematic and layout of the oscillator cell are shown in Fig. 3.1 and Fig. 3.2 respectively. An open loop optimization of the locking range by lowering the $Q$ of the oscillator introduced in [3.9] is performed using Agilent ADS to reduce the phase slope of the open loop gain at 10 GHz.

Table 3.1 provides the optimized oscillator parameters. A Fujitsu FHX35LG HEMT is used as the oscillating device. The transistor is biased with 3V at the drain with the gate at ground. With $R_S$ of 33Ω, this corresponds to $V_{DS}$ of 2.4 V and $I_D$ of 16 mA.

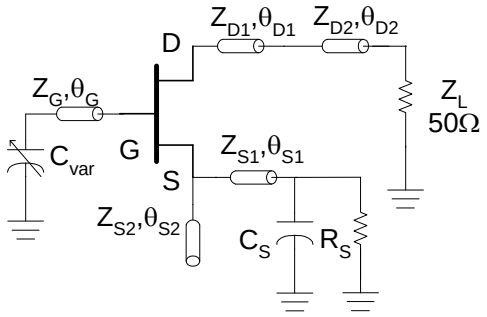


Fig. 3.1 Oscillator schematic.

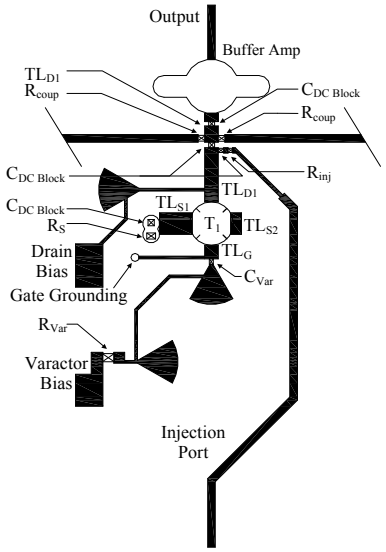


Fig. 3.2 Layout of 10 GHz oscillator cell.

Table 3.1 Oscillator circuit parameters.

| Component Values | | |
|---|---|---|
| Transmission Lines | Length (mil) | Width (mil) |
| $TL_{D1}$ | 100 | 25 |
| $TL_{D2}$ | 30 | 25 |
| $TL_{S1}$ | 60 | 40 |
| $TL_{S2}$ | 20 | 40 |
| $TL_G$ | 10 | 10 |
| Output and Coupling Lines | | 14 |
| Lumped Elements | | |
| $R_S$ | 33 Ohm (w/ bond wire) | |
| $R_{inj}$ | 50 Ohm | |
| $R_{coup}$ | 50 Ohm | |
| $R_{Var}$ | 1 kOhm | |
| $C_{VAR}$ | 0.2-2.0 pF | |
| $C_{DC\ Block}$ | 47 pF (w/ bond wire) | |
| $T_1$ | FHX35LG | |

The small signal S-parameters of the transistor and varactor are measured with a network analyzer and used in the design.

The COA was fabricated on 0.635-mm thick Rogers TMM 10i $(\varepsilon_r = 9.8)$ board and is shown in Fig. 3.3. The oscillators were coupled with 50-$\Omega$ transmission lines with a coupling phase of $\Phi = 4\pi$ at 10 GHz and resistively loaded with 50-$\Omega$ chip resistors. Each oscillator has an injection port which can be terminated either in a 50-$\Omega$ load or with an external injection signal. Each VCO delivers power to a patch antenna through a buffer amplifier. A Narda Microwave $180^\circ$ hybrid coupler (model 4346) is used to provide the phase shifted injection signal to facilitate the multiport injection locking scheme. Theoretically, the sum input port of the coupler provides two signals that are in-phase with each other. This input could be used to measure the broadside pattern of the array. Ideally the delta input port of the coupler provides signals that are $180^\circ$ out of phase with each other and is used for the various multiport injection locking scenarios. The hybrid coupler's performance at 10 GHz was measured using a network analyzer and when the delta input port is used, the output signals are found to have a phase difference of $174^\circ$ and had a transmission loss of 4.5 dB. When the sum input is used, the phase difference between the output signals is $5^\circ$. Hence the hybrid coupler is not used for the broadside pattern measurement. An Agilent 83620B signal generator is used as the injection source. With the cable loss and the 4.5dB loss in the coupler, the maximum available injection signal power is -7dB.

Fig. 3.3 shows the setup where oscillators #1 and #9 are chosen as the locations for multiport injection locking. The injection ports on the other oscillators are terminated in a 50-$\Omega$ load. Two identical cables are used to connect the outputs of the coupler to the oscillators. This is done to ensure that there is no additional phase shift due to cable

length mismatch. Far field pattern measurements are made in an anechoic chamber for different multiport injection locking scenarios.

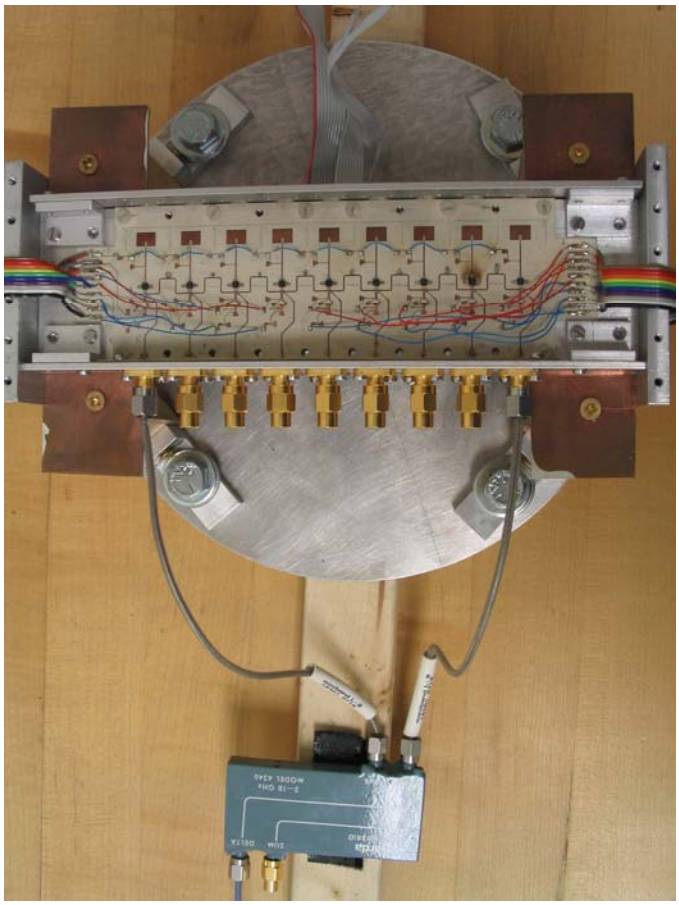

Fig. 3.3 Photograph of the 9-element COA with the 180° hybrid coupler.

## C. COA Radiation Patterns

The radiation patterns are measured for the array at broadside and for the cases when oscillator pairs #1 and #9, #2 and #8, #3 and #7 and #4 and #6 were injection locked with a 174° phase difference. In a linear array, the maximum achievable beam steering $\psi$ for an inter-element phase shift $\Delta\phi$ is computed from [3.10]:

$$\psi = \sin^{-1}\left(\frac{\lambda_0}{2\pi d}\Delta\phi\right) \tag{3.1}$$

where $d$ is the antenna spacing and $\lambda_0$ is the free space wavelength. Injection locking oscillators #1 and #9 with a 174° phase difference results in an inter-element phase shift of 21.75°. For an element to element spacing of .580" and frequency of 10 GHz, using (3.1) the maximum theoretical beam steering is 7°. The coupler output signals are fed to the oscillators #1 and #9 as shown in Fig. 3.3. The frequency detuning scheme was employed to provide steering in both directions. This scheme also provides additional beam steering.

Fig. 3.4 shows the measured radiation patterns under steered conditions when oscillators #1 and #9 are simultaneously injection locked with a 174° phase difference. The broadside pattern is also shown.

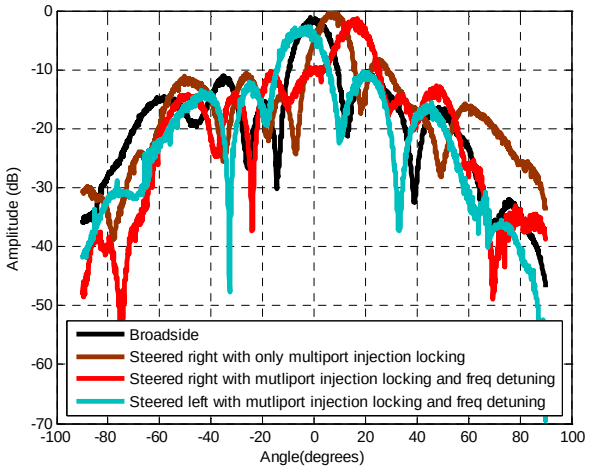


Fig. 3.4 Beam steering with oscillators #1 and #9 injection locked with 174° phase difference.

With multiport injection locking alone the beam is steered to 6.9°, which is close to the

maximum theoretical value of 7°. By frequency detuning the end oscillator elements the beam is further steered to the right by 7° (oscillator #9 tuned to 10.0375 GHz and oscillator #1 tuned to 9.973 GHz) and to the left by 9.1° (oscillator #1 tuned to 10.054 GHz and oscillator #9 tuned to 9.9595 GHz). Thus the total steering obtained by employing both the methods are +13.9° and -2.2° from broadside. Hence additional steering can be obtained by applying the frequency detuning scheme to multiport injection locking.

Simultaneous injection locking of oscillators #2 and #8 with a 174° phase difference, results in a uniform phase progression of 29°, which corresponds to a maximum theoretical beam steering (from (3.1)) of 9.3°. Fig. 3.5 shows the measured radiation patterns.

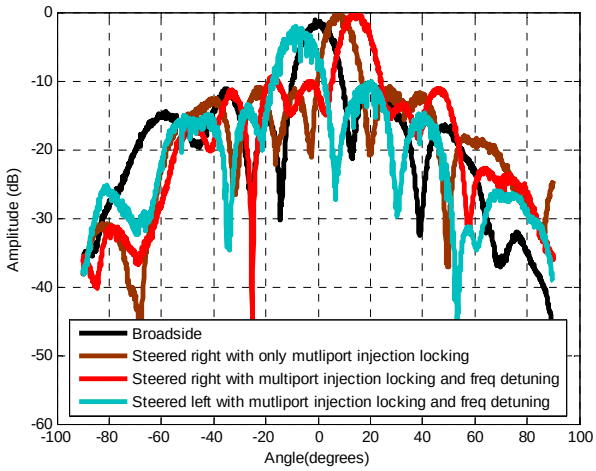


Fig. 3.5 Beam steering with oscillators #2 and #8 injection locked with 174° phase difference.

From Fig. 3.5, one observes that the multiport injection locking scheme alone provides a beam steering of 9.2°, which almost achieves the maximum theoretical steering. The

beam is further steered to the right by 4.7° (oscillator #9 tuned to 10.028 GHz and oscillator #1 tuned to 9.986 GHz) and to the left by 17.2° (oscillator #1 tuned to 10.087 GHz and oscillator #9 tuned to 9.9375 GHz). Thus the total steering obtained by employing both the methods are +13.9° and -8° from broadside.

Moving the injection locking locations to oscillators #3 and #7 results in an inter-element phase shift of 43.5°, which corresponds to a maximum theoretical beam steering of 14° (from (3.1)). Fig. 3.6 shows the measured patterns, from which one observes that the multiport injection locking scheme alone provides a beam steering of 12.6°.

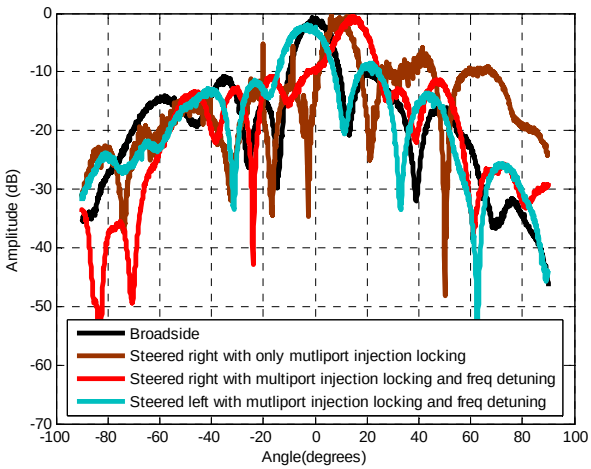


Fig. 3.6 Beam steering with oscillators #3 and #7 injection locked with 174° phase difference.

Frequency detuning the end oscillators (oscillator #9 tuned to 10.007 and oscillator #1 tuned to 9.995 GHz) further steers the beam to the right by 1.2°. The additional beam steering achieved for this case is less than the other two previously discussed multiport injection locking scenarios. This is due to locking range limitations. The beam is steered to the left by 15.5° by detuning oscillator #1 to 10.068 GHz and oscillator #9 to 9.9355

GHz. Therefore with oscillators #3 and #7 simultaneously injection locked with 174° phase difference, the beam total steering achieved by employing both the methods is +13.9° and -2.9° from broadside.

An 87° inter-element phase difference is obtained by simultaneous injection locking of oscillators #4 and #6, which corresponds to a theoretical beam steering of 28.9° (from (3.1)). The measured radiation patterns are shown in Fig. 3.7.

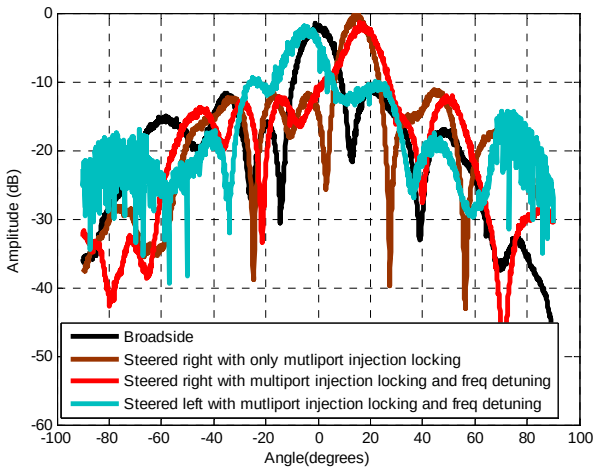


Fig. 3.7 Beam steering with oscillators #4 and #6 injection locked with 174° phase difference.

This multiport injection locking combination provides the largest beam steering of 15.6°. Applying the frequency detuning method along with the multiport injection technique, the beam is only marginally steered further to the right. The beam steering in a COA is limited by the ±90° inter-element phase difference. By frequency detuning the end elements, the inter-element phase difference approaches 90°. The beam is steered 0.5° further to right by detuning oscillator #9 to 10.002 GHz and oscillator #1 to 9.997 GHz. This slight detuning brought the array to the edge of the locking range, which limits the additional steering. The beam is steered left by 20.7° by detuning oscillator #1 to 10.089

GHz and oscillator #9 to 9.9295GHz. Thus the overall steering achieved with this injection locking location is +16.1° and -5.1° from broadside.

Table 3.2 provides a summary of the theoretical and measured beam steering for simultaneous injection locking of multiple oscillator elements with 174° phase difference. Table 3.3 summarizes the theoretical and measured beam steering under maximum steered right and steered left conditions when the frequency detuning and the multiport injection locking schemes are employed simultaneously.

Table 3.2 Summary of theoretical and measured beam steering for simultaneous injection locking with 174° phase difference.

| Oscillators Injection Locked | Inter-element phase difference (degrees) | Theoretical beam steering (degrees) | Measured beam steering (degrees) |
|---|---|---|---|
| 1 and 9 | 21.75 | 7 | 6.9 |
| 2 and 8 | 29 | 9.3 | 9.2 |
| 3and 7 | 43.5 | 14 | 12.6 |
| 4 and 6 | 87 | 28.9 | 15.6 |

Table 3.3 Summary of inferred oscillator phase differences and measured beam steering for application of frequency detuning scheme with simultaneous injection locking.

| Oscillator Injection Locked | 1 and 9 | 2 and 8 | 3 and 7 | 4 and 6 |
|---|---|---|---|---|
| Inferred inter-element phase difference under maximum steered right conditions (degrees) | 43.7 | 43.8 | 48.8 | 88.6 |
| Measured beam steering (degrees) | 13.9 | 13.9 | 13.8 | 16.1 |
| Inferred inter-element phase difference under maximum steered left conditions (degrees) | -28.47 | -53.23 | -48.1 | -63.63 |
| Measured beam steering (degrees) | -9.1 | -17.2 | -15.5 | -20.7 |
| Measured beam steering from broadside (degrees) | +13.9/ -2.2 | +13.9/ -8 | +13.9/ -2.9 | +16.1/ -5.1 |

## III. Use of Multiport Injection Technique for Further Improvement of Array Phase Noise

Tompkins [3.6] extended the phase noise theory developed by Chang *et al.* [3.8] to account for the NBIL phenomenon. The phase noise of an $N$ element array, considering the NBIL phenomenon can be computed from [3.6]:

$$\left|\delta\theta_{total}\right|^2 = \frac{\left|B_n\right|^2}{N^2}\sum_{j=1}^{N}\left|\sum_{i=1}^{N} p_{j,i}\right|^2 + \frac{\left|B_{n,inj}\right|^2}{N^2}\left|\sum_{i=1}^{N} p_{N+1,i}\right|^2 \qquad (3.2)$$

where $\left|B_n\right|^2$ is the power spectral density of the oscillator's quadrature noise source, $\left|B_{n,inj}\right|^2$ is the power spectral density of the quadrature noise component of the injection

source and $p_{j,i}$ is a matrix representing the coupling topology.

Two and three port injection locking of a nine element COA have been shown to provide considerable array phase noise improvement over single port injection locking [3.6]. In their work, oscillators #1 and #9 are chosen as the two port injection locking locations while oscillators #1, #5 and #9 are chosen for three port injection locking. For particular injection signal strength, two and three port injection locking of the array provide a 10 and 15 dB improvement in phase noise respectively over single port injection locking.

The phase noise performance of the array injection locked at multiple oscillators can be further improved by making majority of the injection signal power available near the center element. Two, three and four port injection locking of the nine element array used in [3.6] is performed for various injection locking scenarios. A Microwave Dynamics Phase-Locked DRO with an output power of 13 dBm is utilized as the injection source. A 4 way equal split Wilkinson power divider is employed to facilitate multiport injection locking. Ideally, the divider should have 6 dB loss per port. The divider loss is measured using a network analyzer and is found to be 8-9 dBm. This limited the maximum injection power available to about 5 dBm. Fig. 3.8 shows the photograph of the array with oscillators #1 and #9 connected to the Wilkinson divider network. The injection ports on the other oscillators and the unused divider outputs are terminated with 50-$\Omega$ loads. The phase noise of the array is measured for various multiport injection locking scenarios using an Aeroflex Comstron PN9000B phase noise measurement system for $\rho = -25\,\text{dBm}$. The measured results are compared with the theoretical phase noise

computed from (3.2).

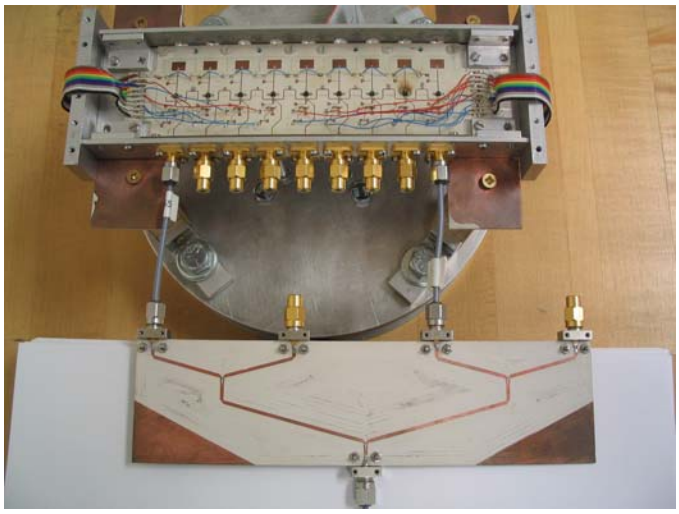

Fig. 3.8 Photograph of the array and the Wilkinson divider network.

Fig. 3.9 shows the measured and theoretical array phase noise for different two port injection locking locations.

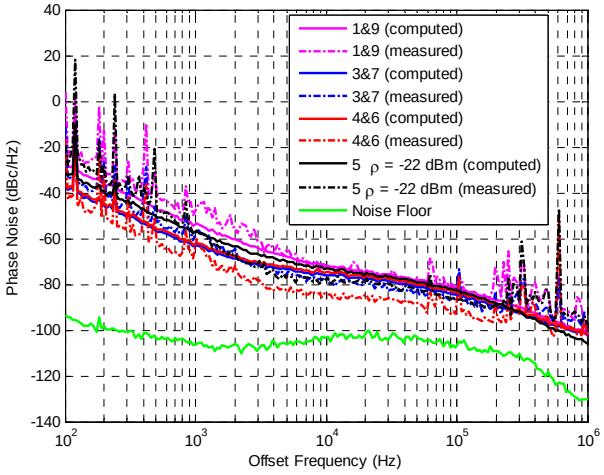


Fig. 3.9 Computed and measured phase noise for different two port injection locking scenarios.

One observes in Fig. 3.9 that moving the injection locking locations progressively towards the center element results in improved phase noise performance. At 10 kHz

offset, injection locking at oscillators #4 and #6 provides a 12 dB improvement over injection locking at oscillators #1 and #9. Injection locking at oscillators #4 and #6 makes majority of the applied signal power available near the center element, which results in an effective distribution of the injected signal power along the array. Fig. 3.9 also gives a comparison of the array phase noise between the various two port injection locking scenarios and injection locking the center oscillator with twice the signal power. It is clear that injection locking at oscillator #5 with twice the signal power provides considerable improvement over the phase noise performance with oscillators #1 and #9 injection locked. When oscillators #4 and #6 are chosen as the two port injection locking locations, the phase noise is slightly better than the single port case with twice the injection signal power. This indicates that injection locking at elements closer to the center element results in more effective injection signal power sharing in the array.

Fig. 3.10 shows the array phase noise when oscillators #1 and #9, #1 and #5, and #4 and #5 are chosen as the injection locking locations.

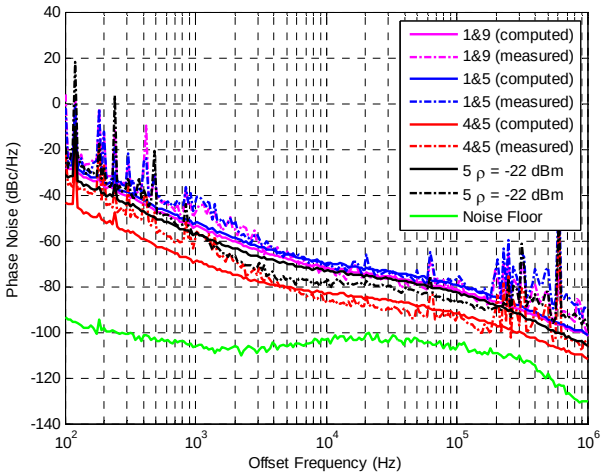


Fig. 3.10 Computed and measured phase noise for different two port injection locking scenarios.

Comparing the different injection locking scenarios depicted in Fig. 3.10, the best phase noise performance is observed when the array is injection locked at oscillators #4 and #5 while the worst is observed for injection locking at oscillators #1 and #9. This shows that if multiport injection is used it is advantageous to injection lock the elements closer to the center element.

Fig. 3.11 and 3.12 present the phase noise performance of the array for different three and four port scenarios respectively.

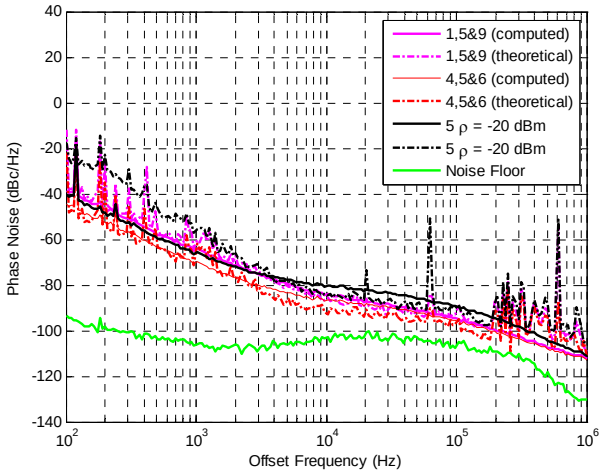


Fig. 3.11 Computed and measured phase noise for different three port injection locking scenarios.

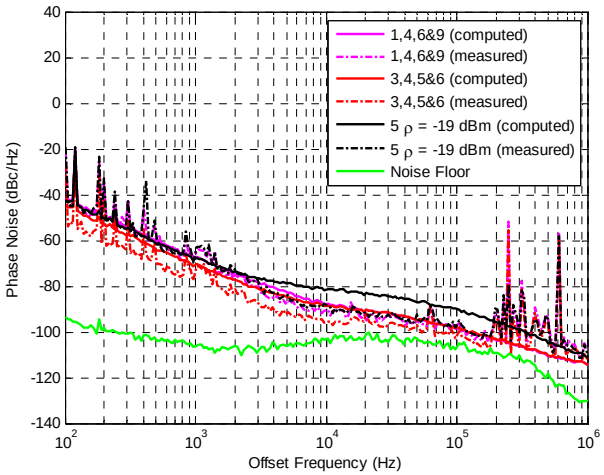


Fig. 3.12 Computed and measured phase noise for different four port injection locking scenarios.

The phase noise performance with oscillators #1, #5 and #9 and oscillators #1, #4, #6 and #9 injection locked is comparable with the performance with thrice and quadruple power at the center element respectively. One observes in Fig. 3.11 and 3.12 that better phase noise performance is obtained when the oscillators closer to the center element are chosen for injection locking, which is in keeping with the two port case.

Fig. 3.13 and 3.14 compare the phase noise of the array for select two, three and four port injection locking scenarios. Fig. 3.13 compares the phase noise of the best two; three and four port injection locking locations whereas Fig. 3.14 contrasts the measured array phase noise performance for select two, three and four port injection locking locations. From these figures, it can be observed that the injection locking location is crucial for phase noise performance when multiple oscillators are injected locked to a source. Fig. 3.14 shows that if multiport injection locking is employed at the center elements, the same phase noise performance can be obtained by injection locking fewer oscillator elements.

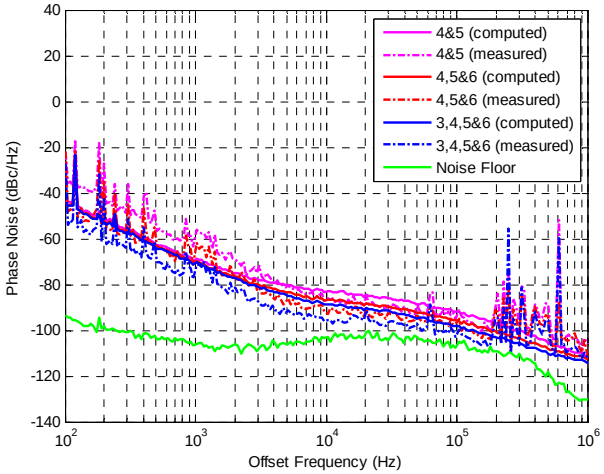


Fig. 3.13 Comparison of computed and measured array phase noise performance for best two, three and four port injection locking locations.

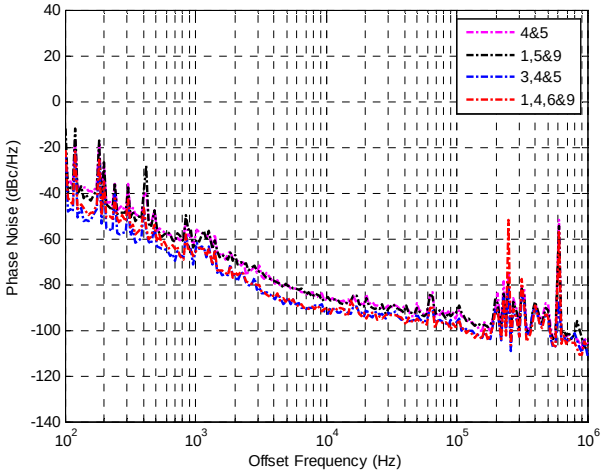


Fig. 3.14 Phase noise performance of array for select two, three and four port injection locking scenarios. Injection locking at oscillators #4 and #5 and oscillators #3, #4 and #5 provide the same phase noise as injection locking at oscillators #1, #5 and #9 and #1, #4, #6 and #9 respectively.

## IV. Conclusion

In this paper, the multiport injection technique is shown as a means to enhance the beam steering and phase noise performance of the array. For a nine element coupled

oscillator array operating at 10 GHz, the maximum beam steering (15.6°) is obtained when oscillators #4 and #6 are simultaneously injection locked with a 174° phase difference. Additional beam steering is observed when the frequency detuning method was employed along with the multiport injection locking technique. Using both the methods, the maximum beam steering is achieved for the above mentioned multiport injection locking scenario and is found to be + 16.1° and -5.1° from broadside. Two, three and four port injection locking of the array is performed and the measured phase noise performance is compared with theory. Regardless of the number of oscillators simultaneously injection locked, the best phase noise performance is observed when the oscillators nearest to the center element are chosen for injection locking. By injection locking the oscillators nearest to the center element it is shown that the same phase noise performance is obtained with fewer injection locked oscillators.


## Acknowledgment

The authors wish to gratefully acknowledge the numerous fruitful technical conversations with Dr. Christopher M. Tompkins of Northrop Grumman Corporation, Baltimore, MD, USA.


## References


[3.1] R. A. York, "Nonlinear analysis of phase relationships in quasi-optical oscillator arrays," *IEEE Trans. Microwave Theory Tech.*, vol. 41, pp. 1799-1807, Oct. 1993.

[3.2] P. Liao and R.A. York, "A six-element beam-scanning array," *IEEE Microwave and Guided Wave Letters,* vol.4, pp. 20-22, Jan.1994.

[3.3] Ronald J. Pogorzelski, Rocco P. Scaramastra, John Huang, Robert J. Beckon, Steven M. Petree, and Cosme M. Chavez, "A seven-element S-band coupled-oscillator controlled agile-beam phased array," *IEEE Trans. Microwave Theory Tech*., vol. 48, pp. 1375-1384, Aug. 2000.

[3.4] K.D. Stephan and W.A. Morgan, "Analysis of inter-injection locked oscillators for integrated phased arrays," *IEEE Trans. Antennas Propagat.,* vol. 35, pp. 771-781, July 1987.

[3.5] K.D. Stephan and S.L. Young, "Mode stability of radiation-coupled inter-injection-locked oscillators for integrated phased arrays," *IEEE Trans. Microwave Theory Tech*., vol. 36, pp. 921-924, May 1988.

[3.6] Christopher Tompkins, "Coupled oscillator array design and the use of multiport injection locking for improved performance," Ph.D. dissertation, Dept. Elect. Comput. Eng., Clemson University, SC, 2006.

[3.7] H. C. Chang, X. Cao, M. J. Vaughan, U. K. Mishra, and R.A. York, "Phase noise in externally injected-locked oscillator arrays," *IEEE Trans. Microwave Theory Tech*., vol. 45, pp. 2035-2042, Nov. 1997.

[3.8] H. C. Chang, X. Cao, U. K. Mishra, and R. A. York, "Phase noise in coupled oscillators: theory and experiment," *IEEE Trans. Microwave Theory Tech*., vol. 45, pp. 604-615, May 1997.

[3.9] X. Wang and L. W. Pearson, "Design of coupled-oscillator arrays without a posteriori tuning," *IEEE Trans. Microwave Theory Tech*., vol. 53, pp. 410-413, Jan. 2005.

[3.10] W. L. Stutzman and G. A. Thiele, *Antenna Theory and Design*. New York: Wiley, 1981.

# CONCLUSIONS

The dissertation focuses on improving the mutual injection locking range (MILR), phase noise characteristics and beam steering capabilities of coupled oscillator arrays (COAs). In the first paper, the effect of the coupling phase on the mutual injection locking range was investigated. The type of resonance, series or parallel, presented to the coupling network depends by the oscillator circuit depends upon the coupling point in the oscillator circuit. Two, three-element COAs operating at 3.75 GHz were fabricated -one in which oscillators were mutually coupled at the drain terminal and another in which oscillators were mutually coupled at the gate terminal. It was shown that the coupling phase that resulted in broadside operation yielded the largest MILRs, whereas the coupling phase that caused the array to lock with a limited range resulted in out of phase synchronization of the oscillator elements.

In the second paper, the dynamics of strongly coupled oscillator arrays were examined. The breakdown of the broadband condition in the strongly coupled regime was shown. A five-element COA operating at 3.75 GHz was fabricated and the MILR, phase noise and oscillator amplitude and phase variation were measured for coupling strengths varying from 0.5 to 2.5. Two-fold improvement in the MILR and 25 dB improvement in the array free-running phase noise was achieved. Strongly coupled arrays were shown to operate closer to the noise floor with less injection power. Upon strong coupling the amplitudes of the oscillator elements were shown to grow toward the extremes of the array. The oscillator amplitudes were tapered and reduction in the side lobe level was achieved at the expense of beam directivity and effective isotropic radiated power. The

beam steering capabilities of strongly coupled arrays were also presented.

The third paper employed multiport injection locking to show improvement in the beam steering and phase noise characteristics of a nine-element COA operating at 10 GHz by moving the injection locking locations progressively towards the center oscillator element. It was shown that the maximum steering of the beam from broadside was achieved when oscillators #4 and #6 were injection locked with a $174^{\circ}$ phase difference. The phase noise performance of the array was evaluated for various two, three and four port injection locking scenarios and the best performance was observed when oscillators #4&#5, oscillators #3, #4&#5 and oscillators #3, #4, #5&#6 respectively were chosen as the injection locking locations. It was shown that by injection locking the oscillators near the center oscillator, the same phase noise performance could be obtained with fewer injection- locked oscillators.

Currently, coupled oscillator arrays are realized using hybrid circuit fabrication. Differences in the oscillator free-running frequencies, which arise due to cell-to-cell component variation, remain as one of the main concerns inhibiting the implementation of COA architecture in phased array systems. Voltage controlled oscillators are utilized as the unit oscillators allowing for post tuning to reduce the difference in the free-running frequencies.

Fabrication of COAs using modern MMIC technology could springboard COAs as a low cost alternative to complex phased array systems. However, the requirement of post tuning techniques for controlling the difference in the oscillator free-running frequencies makes the task arduous. Post tuning techniques such as laser trimming would

reduce the potential cost savings sought from the MMIC approach. Alternatively, wide locking range oscillators help in achieving good array performance in spite of the variations in the free-running frequencies. Strong coupling between the oscillators helps in widening the mutual injection range. Thus, strongly coupling can be utilized in COAs to alleviate the adverse effects caused by the variation in the free-running frequencies. Strongly coupled oscillators could be pursued further to realize COAs using the MMIC approach. However, substantial resources are required to pursue the MMIC approach.

# APPENDIX

## Finite Difference Approximation Technique for Solving Coupled First-Order Differential Equations

The time-domain dynamic equations of coupled oscillator arrays can be generalized to a set of *N* coupled first-order ordinary differential equations of the form

$$\frac{dy_i}{dx} = f_i\left(x, y_i, ...., y_N\right), \qquad i = 1, 2, .....N, \tag{A.1}$$

where the functions $f_i$ are known, and the initial values of $y_i$ at the starting value $x_0$ are also known. This set of equations can be solved using a finite-difference (FD) approximation [A.1]. Fig. A.1 shows the various FD approximations of the first derivative, $f'(x)$.

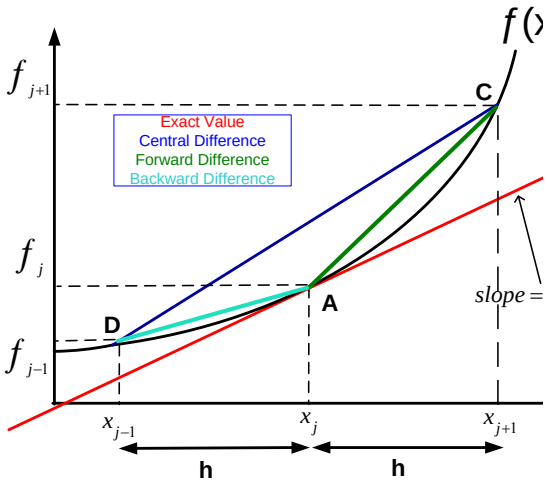


Fig. A.1 Finite-difference approximations to f'(x).

FD approximations of derivatives replace the terms in the differential equation by terms involving algebraic operations only. Using Taylor's theorem with remainder, the various approximations to the first derivative are given by (A.2),

$$
\begin{aligned}
f'(A) &= \frac{f(x_j) - f(x_{j-1})}{h} = \frac{f(A) - f(D)}{h}, \quad \text{backward difference} \\
f'(A) &= \frac{f(x_{j+1}) - f(x_j)}{h} = \frac{f(C) - f(A)}{h}, \quad \text{forward difference} \\
f'(A) &= \frac{f(x_{j+1}) - f(x_{j-1})}{2h} = \frac{f(C) - f(D)}{2h}, \quad \text{central difference}
\end{aligned}
\tag{A.2}
$$

where h is the time step.

The backward difference approximation is applied to solve (2.9) and (2.13) through an iterative process. The initial value of the free running oscillator amplitude and phase are chosen as 1 and 0 respectively. In each iteration, the time is advanced by an interval of 0.001. The process is continued until the error between two successive iterations is smaller than 0.0001.

## References


[A.1] A. Taflove and Susan C. Hagness, *Computational Electrodynamics: The Finite-Difference Time-Domain Method, 2nd ed.*, Boston: Artech House, 2000.